Lawrence Berkeley National Laboratory
Recent Work

Title

Microstructure Influences on the Mechanical Properties of Solder

Permalink

https://escholarship.org/uc/item/8vv9f767

Authors

Morris, J.W.
Freer, J.L.
Mei, Z.

**Publication Date**

1993

Center for Advanced Materials

CAM

Presented at the Third International Workshop on Materials
and Mechanics Issues of Solder Alloy Applications, Santa Fe, NM,
September 9–11, 1992 and to be published as a chapter in
The Mechanics of Solder Alloy Interconnects, S.N. Burchett,
D.R. Frear, H.S. Morgan, J.H. Lau, Eds.,
Van Nostrand Reinhold, New York, NY, 1993

Microstructural Influences on the Mechanical Properties of Solder

J.W. Morris, Jr., J.L. Freer Goldstein, and Z. Mei

April 1993
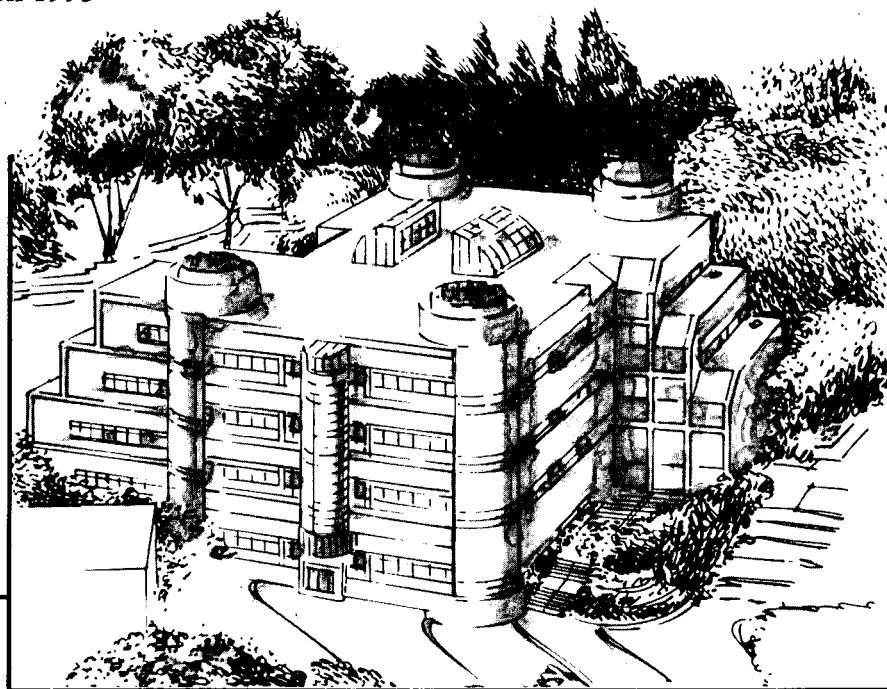
Materials and Chemical Sciences Division

Lawrence Berkeley Laboratory • University of California

ONE CYCLOTRON ROAD, BERKELEY, CA 94720 • (415) 486-4755

DISCLAIMER

DISCLAIMER

MICROSTRUCTURAL INFLUENCES ON THE MECHANICAL PROPERTIES OF SOLDER

J.W. Morris, Jr., J. L. Freer Goldstein and Z. Mei

Department of Materials Science and Mineral Engineering
University of California

and

Center for Advanced Materials
Materials Sciences Division
Lawrence Berkeley Laboratory
University of California
Berkeley, CA 94720

April 1993

MICROSTRUCTURAL INFLUENCES ON THE MECHANICAL PROPERTIES OF SOLDER

J.W. Morris, Jr., J.L. Freer Goldstein and Z. Mei

Department of Materials Science, University of California, Berkeley, and
Center for Advanced Materials, Lawrence Berkeley Laboratory

INTRODUCTION

The main intent of this book is to review analytic methods for predicting the behavior of solder joints. These are based on continuum mechanics. The solder is treated as a continuous, homogeneous body, or composite of such bodies, whose mechanical behavior is uniform and governed by constitutive equations that are simple enough to produce mathematically tractable models.

However, it is well known that real solids, and particularly solder joints, are not continuous media. They are microcomposites with complex microstructures. The constitutive equations that are used to describe their behavior are macroscopic relations that predict the cumulative effect of complex deformation processes that occur on the microstructural level. At the present state of the science it is not possible to construct tractable theories that incorporate the microstructure directly. However, it is important to recognize that the microstructure exists, and that it is ultimately responsible for the macroscopic behavior that is modeled.

The microstructure of a solder joint influences its mechanical properties in three generically different ways.

• The microstructure governs deformation and failure.

The normal mechanical properties of a solder joint depend on the motion of dislocations and the growth and reconfiguration of grains. The processes are more sensitive to the microstructure of the solder than to its chemical composition. Since a joint of given composition may have any one of several qualitatively different microstructures, depending on how it is solidified, aged or deformed, the microstructure must be given, at least implicitly, as part of the specification of the material that underlies the choice of a particular constitutive relation to describe its mechanical properties. There is no such thing as *the* mechanical behavior of a particular solder; it depends on the microstructure, which depends, in turn, on how the solder is processed.

• Common solders deform inhomogeneously.

Solder joints ordinarily have complex microstructures, are used at high homologous temperatures, and deform under relatively low loads. These three factors have the consequence that the plastic deformation of a solder joint is rarely uniform. It is concentrated in well-defined shear bands that are accentuated as deformation proceeds. From the macroscopic perspective, solder often exhibits strain-softening. This is not necessarily because the solder inherently softens (though it may) but because the inhomogeneous pattern of the deformation has the consequence that very little of the solder volume actually participates in plastic deformation. From the microscopic perspective, it is insufficient to know the local mechanical properties of the solder. One must also have a sense of how the inhomogeneous deformation pattern develops.

• Common solders are microstructurally unstable.

Good solders are low-melting alloys and, hence, are ordinarily eutectics or other two-phase mixtures. They bond to the substrate by reacting chemically to form intermetallic compounds. They are ordinarily used in the as-solidified or slightly aged condition. These factors ordinarily lead to a microstructure that is thermodynamically unstable. As the joint is aged, thermally cycled or deformed, its microstructure evolves so that its mechanical behavior changes with time.

In the following we shall develop these principles by briefly reviewing the variety of microstructures that are often found in solder joints, and discussing some of the ways in which the microstructure influences the common types of high-temperature mechanical behavior. We shall not attempt to be comprehensive. A great many different solder compositions are used in modern electronic devices, only a few of which have been studied in metallurgical detail.

SOLDER MICROSTRUCTURES

The most common solder joints contain Pb-bearing solders (Sn-Pb, Sn-In, Sn-Bi, Sn-Ag, or ternaries of these) that join surfaces that are predominantly Cu or Ni, and may be coated with Au. We first consider the microstructure of the solder itself, and then consider the changes that are caused by its reaction with the metallization at the interface.

Pb-Sn solder joints provide a good general model, since they exhibit most of the important types of behavior that are found in general in solder joints.

The Pb-Sn binary phase diagram is drawn in Fig. 1. It is of a type that is called a simple eutectic phase diagram, since the lowest value of the melting point of the system falls at a eutectic point where the liquid solidifies into a mixture of two solids, α, a Pb-rich solid solution, and β, a Sn-rich solid solution. The other common Sn-bearing solders have phase diagrams that resemble this one in their most pertinent details.

The microstructures that result from solidification in a system that has a phase diagram like that shown in Fig. 1 depend on the composition of the liquid and the rate at which the liquid is cooled. The influence of composition can be described in terms of the three typical cases that are indicated in Fig. 1: eutectic (labeled (1) in the figure), off-eutectic (labeled (2)), and solvent-rich (labeled (3)).

Eutectic microstructures

If a material with a eutectic composition (labeled (1) in Fig. 1) is solidified by cooling relatively slowly it forms a microstructure like that shown in Fig. 2. The two solid solutions that make up the eutectic grow simultaneously and parallel to one another in grain-like colonies like those shown in the figure.

If the two phases are present in roughly equal volume fraction, they form parallel plates within each colony. If one phase predominates, the second ordinarily forms rods in the matrix of the other. The former case is illustrated by the Sn-Bi eutectic that is shown in Fig. 3a [1]. The latter case is illustrated by the Sn-In eutectic shown in Fig. 3b [2]. When one phase is very strongly predominant the second may appear in the form of acicular needles, as seen in the Sn-Ag eutectic in Fig. 3c [3].

The eutectic microstructure is often complicated by precipitation within one or both of the eutectic constituents when the sample is cooled below the eutectic solidification temperature. This phenomenon is observed, for example, in the Sn-Pb [4] and Sn-Bi eutectics. As illustrated in Fig. 4, small Bi-rich particles form within the Sn-rich phase [3]. This secondary precipitation is due to the fact that the solubility of Bi in Sn decreases significantly as temperature is lowered below the eutectic point. When a eutectic solder is cooled below its eutectic point, the Sn-rich constituent becomes increasingly supersaturated with Bi. The supersaturation is relieved by the precipitation of Bi-rich phases within the Sn-rich phase.

The eutectic microstructure has a very high surface area per unit volume, and is, therefore, thermodynamically unstable with respect to reconfiguration into a mixture of coarser or more equiaxed grains. If a freshly solidified eutectic is simply aged at moderate temperature, the phases grow, and eventually rearrange themselves into an equiaxed structure. In most cases this process is dramatically accelerated by plastic deformation. In Pb-Sn and many other eutectics, accumulated plastic deformation couples with the large surface area to promote recrystallization into a microstructure of fine, equiaxed grains. The recrystallized structure of the Pb-Sn eutectic is illustrated in Fig. 5 [5]. Once the structure has recrystallized, the grains gradually increase in size to further decrease the surface area per unit volume.

A eutectic structure that strongly resembles the recrystallized microstructure can be obtained directly by cooling quickly from the melt. When solidification happens quickly under substantial undercooling, the classic eutectic structure is suppressed and the material solidifies directly into an equiaxed two-phase mixture. The structure of rapidly solidified Pb-Sn is illustrated in Fig. 6 [5].

Off-eutectic microstructures

The vertical line labeled (2) in Fig. 1 is an example of an off-eutectic composition. When a solder of this composition is solidified by cooling at a slow to moderate rate, the α-phase forms as discrete islands at temperatures within the $\alpha+L$ field. The liquid that remains when the eutectic temperature is reached solidifies into the eutectic microstructure. The final microstructure resembles that shown in Fig. 7, with islands of pro-eutectic phase embedded in a matrix of eutectic [6].

Precipitated microstructures

A composition like that labeled (3) in Fig. 1 leads to a qualitatively different microstructure. A solder of this composition solidifies into a polygranular microstructure of a single phase (α in the example given in the figure). On further cooling, the solder penetrates the two-phase ($\alpha+\beta$) region, which causes the precipitation of particles of β-phase within the matrix of α. 95Pb-5Sn is a widely used solder that has this solidification behavior.

When precipitated microstructures are aged at relatively high homologous temperatures, both the primary α grains and the embedded β precipitates gradually coarsen. If the microstructure is thermally cycled, however, it may exhibit more dramatic instabilities. If the solubility of the minor species is a strong function of temperature, as it is in Pb-rich Pb-Sn solders, for example, then the volume fraction of precipitate decreases rapidly on heating, and increases on cooling. A periodic thermal cycle causes the periodic dissolution and re-precipitation of solute, and may lead to the reconfiguration of the precipitate phase into grain boundaries or regions of high internal stress.

Similar instabilities are observed if the material is stressed at high temperature. If the solute-rich precipitate causes a volume or shape change when it forms, then a reconfiguration of the precipitate distribution causes a mechanical strain. At high temperature solute diffusion is relatively rapid, and the precipitate distribution may change in a way that serves to relax the imposed stress.

Intermetallics at the interface

The composition of a solder is chosen so that it forms a strong bond to the metal surfaces it is intended to join. Bonding is promoted by chemical reactions between the solder and the substrate that form intermetallic compounds. The most common interfacial intermetallics are Cu-Sn and Ni-Sn compounds that are formed by reaction between Sn in the solder and Cu or Ni in the substrate.

The most thoroughly studied intermetallics are the Cu-Sn compounds that form when Sn-Pb solders wet Cu. There are two common compounds: Cu_3Sn and Cu_6Sn_5. Cu_3Sn forms preferentially when there is an excess of Cu; for example, it is often found at interfaces between Cu and Pb-rich solders such as 95Pb-5Sn. Cu_6Sn_5 forms preferen-

tially in excess Sn, and is, therefore, the usual interfacial intermetallic in eutectic Pb-Sn solder joints (63Sn-37Pb) and at Cu-Sn interfaces. Since Cu_3Sn is stable at higher temperatures than Cu_6Sn_5, it is also found at interfaces that were exposed to Sn-bearing solders at high temperature. If a relatively thick intermetallic layer is formed by reacting eutectic Pb-Sn with Cu, as happens when a joint is reflowed for significant time or when it is aged after solidification at a temperature near the melting point, the intermetallic layer is often a composite, with Cu_3Sn at the Cu interface and Cu_6Sn_5 at the solder interface (Fig. 8) [7]. The relative amounts of the two intermetallics increase with the growth temperature in a predictable way [8].

The morphology of the intermetallic layer reflects the crystal structure of the intermetallic. Cu_3Sn is orthorhombic in structure, and tends to form a tightly coherent layer with nearly equiaxed grains, as illustrated in Fig. 9 [9]. Cu_6Sn_5 is hexagonal, and tends to form a rough layer with knobs or hexagonal prisms that extend into the solder, as illustrated in Fig. 10 [10].

Intermetallics within the bulk

In addition to the intermetallic layer that forms at the wetted interface, intermetallic phases are also often found within the bulk of the solder joint. These bulk intermetallics have two common sources.

First, intermetallics of the type that form at the interface may also be found in the bulk. The most common examples are the Cu-Sn intermetallics. Long, hexagonal rods of Cu_6Sn_5 are sometimes found in solders immediately after solidification [10]. An example is shown in Fig. 11. These apparently grow from the interface into the molten solder and break away into the bulk while the solder is still molten. Intermetallics also form ahead of the interface during the aging of Cu joints with thin, pre-tinned layers [8]. An example is shown in Fig. 12. In this case, the intermetallic is due to Cu diffusion into the solder, which gradually creates a supersaturated condition.

Second, when Au films are used to protect the substrate prior to wetting, Au-based intermetallics appear within the bulk of the solder. These typically form while the solder is still molten; Au dissolves into the solder and reacts with Sn (or In, in the case of In-Sn solders) to form intermetallics. An example is the dense distribution of $AuSn_4$ intermetallics shown in Fig. 13, which formed when a Cu substrate protected by Au was wet with a eutectic Pb-Sn solder [11]. If the Au layer is not completely dissolved by molten solder during wetting, Au-rich intermetallics continue to grow in the solid state until the layer is consumed. An example in which Sn-In partially wets Au is shown in Fig. 14.

Changes in the solder through intermetallic formation

The formation and growth of intermetallic precipitates changes the composition of the solder by depleting it of the constituent that joins the intermetallic. If the intermetallic forms while the solder is still molten the composition change may change the solidified

microstructure of the solder. For example, if eutectic Sn-Pb wets a Au-coated interface the composition of the molten solder shifts to the Pb-rich side of the eutectic value, and the solidified solder contains islands of pro-eutectic Pb as well as Au-Sn intermetallic precipitates. When the intermetallic (Cu-Sn for example) grows in the solid state, the depletion of Sn creates a Pb-rich layer ahead of the growing intermetallic, and produces a chemically inhomogeneous solder.

THE INFLUENCE OF MICROSTRUCTURE ON MECHANICAL PROPERTIES

The mechanical properties that are important to the service behavior of solder joints include their resistance to fatigue under the thermal excursions encountered during normal operation and their resistance to deformation and fracture during installation and transport. Since the melting points of common solders are only slightly above room temperature, the deformation mechanisms that govern these properties are high-temperature mechanisms, such as creep, recrystallization and recovery. In the following we illustrate how the microstructure affects these properties by reviewing examples of microstructural influences on high-temperature creep, fatigue, and overload fracture.

Creep

Because solders are used at high homologous temperatures, creep deformation plays a role in almost all aspects of their mechanical behavior. A typical high-temperature creep curve is illustrated in Fig. 15[12], which shows how the plastic strain increases with time under constant applied stress. The creep response is conveniently divided into three regimes, called primary, steady-state, and tertiary creep. During primary creep the strain rate decreases with strain, reaching a steady-state value that is preserved for some period of time, but eventually begins a monotonic increase that leads to fracture. The parameter that is most commonly used to characterize creep behavior is the steady-state creep rate, which ordinarily obeys an equation of the form [13]

$$\dot{\gamma} = A\tau^n \exp[-Q/kT] \tag{1}$$

where $\dot{\gamma}$ is the shear strain rate, τ is the shear stress, n is called the stress exponent, and Q is an activation energy. The stress exponent and the activation energy change with the dominant creep mechanism, and may have different values in different regimes of the applied stress.

The microstructure affects the steady-state creep rate in two ways. It influences the pre-factor, A, and it governs the range of stress over which particular creep mechanisms dominate at given temperature.

High-stress creep mechanisms

At sufficiently high stresses all metals creep by a mechanism whose rate is determined by the motion of dislocations through the bulk of the crystal grains. While the

micromechanical details of this universal creep mechanism are still not well understood, it leads to a high stress exponent (n in the range 3-7) and has an activation energy that is close to that for self-diffusion in the bulk, which suggests that dislocation climb is the critical step in the process. The values of n and Q that pertain to this process are sensitive to composition, but do not ordinarily have a strong microstructural dependence.

The absence of a strong microstructure effect in this creep regime is consistent with the deformation mechanism. If the deformation rate is controlled by the resistance to dislocation motion in the interiors of grains, then this step must be slow compared to the processes that transmit strain from grain to grain. As a consequence, the strain rate is relatively insensitive to microstructural details.

The creep properties that remain sensitive to microstructure at high stresses are the transition to tertiary creep and the total elongation to failure. At least two different mechanisms govern the transition to tertiary creep: the onset of cavitation damage at grain boundaries, and plastic instability leading to inhomogeneous deformation.

Microstructural influence on elongation at high stress

Cavitation is largely responsible for tertiary creep in bulk solder samples that are tested in tension. Cavities nucleate, primarily at three- or four-grain junctions, grow with strain, and join to cause failure. This process is promoted by increased grain size, which increases the stress concentration at grain junctions, by irregular grain shapes, which provide sites of unusual stress concentration, and by intergranular precipitates, which constrain deformation at grain boundaries. Hence the elongation is sensitive to the microstructure.

Plastic instability is often responsible for tertiary creep of solder samples that are tested in shear. The strain in these samples becomes progressively inhomogeneous through the development of well-defined shear bands. Particularly at low strain rates, these tend to follow planes of microstructural weakness in the material, such as phase boundaries and colony boundaries in eutectic materials (Fig. 16). The development of inhomogeneous shear bands is especially pronounced in solders that have unstable, eutectic microstructures that are easily recrystallized, such as the Sn-Pb [10] and Sn-Bi eutectics [1]. In these materials, incipient shear bands cause recrystallization, leading to the development of the well-defined recrystallized bands that are commonly observed in eutectic Sn-Pb solders that are crept or fatigued in shear (Fig. 17) [10]. However, plastic instability also develops in soft solders, such as the Sn-In eutectic, that do not undergo obvious recrystallization. In this case shear bands develop, but are not decorated with recrystallized material.

Unlike tertiary creep induced by cavitation, tertiary creep due to plastic instability does not necessarily lead to rapid failure. Soft solders tested in shear often have very large tertiary strains. As illustrated in Fig. 15, even the Sn-Bi eutectic, which is one of the hardest of the low-melting-point solders, undergoes over 50% of its creep strain to failure at 20°C in the tertiary regime [12].

The onset of plastic instability can be delayed by modifying the microstructure to inhibit the development of shear bands. At least three mechanisms are known to be effective: refining the grain size, which tends to homogenize the deformation [5], adding chemical species that disrupt the development of eutectic colonies [10] and introducing pro-eutectic grains or precipitate particles that disrupt the growth of shear bands [6,14].

Intergranular creep

The most striking effect of solder microstructure on creep is the intrusion of inter-granular creep when the microstructure is fine-grained, the stress is low and the temperature is high. The intergranular creep mechanism changes the creep behavior in two ways. First, the intergranular creep mechanism has a stress exponent (n, equation (1)) near 2, and an activation energy that is approximately 50% lower than that observed at higher stresses, and is close to the activation energy for grain boundary diffusion. Second, the intergranular creep mechanism leads to a very stable and non-damaging plastic deformation. This creep mechanism is responsible for the most dramatic type of superplasticity, in which a material undergoes creep strains of several hundred percent prior to failure.

The principal microstructural requirement for intergranular creep is that the grain size be small, nearly equiaxed, and sufficiently stable that it is preserved during deformation. When this is the case, the material deforms primarily by grain boundary sliding, in which grains are displaced with respect to one another by slipping along the boundary between them. The importance of a high grain boundary density is reflected in the constitutive equation for intergranular creep. The pre-factor, A, in this equation decreases with the grain size approximately as d^{-2}. Intergranular creep is negligibly slow unless the mean grain size is less than a few microns.

Since grains are three-dimensional objects, it is impossible to deform an intact material by grain boundary sliding alone. The grain boundary sliding mechanism must act in series with a bulk deformation mechanism that maintains contact along the boundaries and, particularly, along three-grain junction lines. This bulk mechanism is not well understood, but, at least in the case of eutectic Sn-Pb, it obeys a constitutive law of the form (1) with $n \approx 3$ and Q equal to the activation energy for bulk diffusion. The rate of creep is governed by the slowest of mechanisms that act in series. Since the bulk mechanism has a higher stress exponent, it dominates at low stress and limits the range of stresses over which intergranular creep is observed.

The combination of the three creep mechanisms leads to a steady-state creep relation like that shown in Figs. 18 (a) and (b)[15], which are taken from research on recrystallized eutectic Sn-Pb, with the dominant creep mechanism changing from the high-stress creep mechanism to intergranular creep to the compatible bulk creep mechanism as the stress is lowered. However, since the low-stress bulk creep mechanism has a higher activation energy than the intergranular creep mechanism, the intergranular creep regime is gradually pinched off as the temperature decreases. Intergranular creep

only appears at intermediate stresses, only when the temperature is high, and only when the grain size is small.

Microstructural effects in intergranular creep

The classic method for obtaining a material that exhibits intergranular creep, and, hence, superplastic behavior, is to recrystallize a eutectic to obtain a fine, equiaxed grain structure that is stabilized against grain growth because the grains are a fine mixture of two different phases. Eutectic Sn-Pb and eutectic Sn-Bi solders are two of the systems in which this is most easily accomplished. As a consequence, they have been extensively studied as prototypic examples of superplastic materials. More recently, it has been realized that similar microstructures can be achieved by solidifying the eutectic at a sufficiently rapid rate, and that the necessary solidification rates are naturally achieved in eutectic Sn-Pb during the normal processing of small solder joints [16]. Further work has shown that small joints of Sn-In eutectic solidify in a microstructure that exhibits intergranular creep at temperatures above about 60°C, and that non-eutectic solders such as 40In40Sn20Pb also form and maintain fine-grained microstructures that exhibit intergranular creep [17]. On the other hand, fine-grained microstructures are difficult to achieve in Sn-Bi eutectic solders by solidification; these develop a more regular eutectic microstructure when they are solidified at rates that are typical for solder processing [12].

The fine-grained microstructures that lead to intergranular creep have the advantage of providing exceptional creep ductility. As we shall discuss below, they also have excellent fatigue resistance. The disadvantage is that they are unstable with respect to grain growth. Grain growth will cause a gradual deterioration in creep properties and a gradual change in the constitutive equation that governs creep behavior [2]. The rate of grain growth increases with the temperature at which the solder is used, and is also affected by the microstructure, since grain growth is inhibited in a fine, two-phase mixture. To further complicate the issue, deformation of the solder, for example, by thermal excursions during service, can induce a recrystallization that refines the grain size and re-establishes intergranular creep [18].

Intergranular creep can also be suppressed by the introduction of precipitates or dispersants into the solder matrix, including the formation of pro-eutectic grains. An example that is important in practice concerns the use of eutectic solders on Au-coated substrates. As discussed earlier, the gold dissolves into the solder when it is molten and forms intermetallics. These intermetallics decorate the matrix (as illustrated in Fig. 13) and, if the net Au concentration is appreciable, change the composition of the solder by depleting the constituent that participates in the intermetallic. The formation of a dense distribution of intermetallics, like that shown in Fig. 13, suppresses intergranular creep in eutectic Sn-Pb [14], even when the Sn depletion is not great enough to make a dramatic change in the underlying microstructure. A higher Au concentration would deplete the solder of Sn, promoting the formation of large islands of Pb-rich phase that would also suppress intergranular creep.

The dramatic changes in creep properties that are introduced by the rapid solidification or grain refinement of many common solders are a serious barrier to the accurate prediction of mechanical behavior in service. The initial properties of the solder depend on its solidification rate, and, hence, vary with the size, location, thermal treatment, and interface metallurgy of solder joints. These properties then change during service, in ways that depend on both the thermal and mechanical history of the joint. At the present state of knowledge, it is not possible to represent these phenomena in an accurate analytic theory. However, it is important to recognize their importance, and to use that knowledge in the construction of approximate models and in the design of accelerated service tests.

Fatigue

Failure induced by thermal fatigue is one of the most important threats to the integrity of solder joints. The source of the fatigue load is the thermal cycle the joint experiences during service, as the device is turned on and off, or as the temperature of the environment changes. In many cases the strain cycle is predominantly in shear. In almost all cases the joint is cycled at a high homologous temperature, so the cyclic deformation that causes fatigue is largely creep.

Most of the mechanistic studies that have been done on the creep fatigue of solder materials have used fatigue tests that have involved cyclic shear loads on model solder joints [19,20], cyclic tensile loads on model joints[21] or cyclic tensile loads on bulk solder specimens [22]. Most of the work has been done under isothermal conditions, though thermal fatigue studies are also included. It is the authors' biased view that the cyclic shear of model joints provides the best representation of the service behavior of typical solder joints; at least, it produces the types of metallurgical damage that are revealed by post-mortem analysis of simulated service failures.

Fatigue mechanisms in shear

The high-temperature fatigue of solder joints in cyclic shear is strongly affected by the heterogeneity of creep deformation. As discussed above, the creep deformation of typical solders in shear tends to be concentrated in well-defined shear bands. Cyclic shear deformation in fatigue is concentrated in such bands, and eventually leads to crack nucleation and failure. In almost all cases studied to date, creep fatigue damage is located within the bulk solder. While the shear bands that lead to failure may lie close to the interface, the brittle intermetallic layer at the interface does not ordinarily participate in failure unless it so thick that it essentially bridges the solder joint, or unless it is internally flawed.

The shear fatigue mechanism in 63Sn-37Pb with the eutectic microstructure is particularly well documented [10, 23-25]. In this case the concentration of shear within planar shear bands causes recrystallization of the Sn-Pb eutectic, which replaces the eutectic microstructure with a fine-grained, equiaxed material that gradually coarsens as fatigue progresses. The cyclic strain is concentrated within this recrystallized material, and the joint eventually fails along shear bands as illustrated in Fig. 19. Bands of coarsened,

equiaxed grains that resemble these are observed in eutectic Sn-Pb joints that failed in service or under simulated service conditions [26-28].

Reasonably well-defined shear bands form during the fatigue of most coarse-grained solders, but are not always accompanied by recrystallization, even when the initial microstructure is eutectic. For example, the 58Bi-42Sn eutectic recrystallizes within shear bands, while the 52In-48Sn eutectic apparently does not [1].

The development of damage in inhomogeneous shear bands has important implications for both the analysis of solder fatigue and the metallurgical search for fatigue-resistant solders. From the analytic perspective it has the consequence that only a small fraction of the solder cross-section actually participates in cyclic deformation, and undergoes strain cycles that are much larger than the nominal strain on the joint. At least a few analytic studies have attempted to account for this phenomenon, and have shown its importance for fatigue life [29]. Of course, the analytic problem is complicated further if the sheared material recrystallizes, since this changes the mechanical properties of the material that experiences strain.

Metallurgical routes to improved fatigue resistance in shear

The observation that strain concentration in shear bands leads to failure suggests how the fatigue resistance may be improved. If the concentration of shear can be minimized or suppressed, fatigue resistance should increase substantially. Three microstructural approaches have been used to accomplish this: the production of fine-grained microstructures that exhibit intergranular creep, the use of chemical additives to disrupt the microstructure and the addition of dispersants to interrupt shear bands.

The most successful of these is the fine-grained microstructure, which can be produced by rapid solidification, and is naturally achieved in many small solder joints. While there has been very little research on the creep fatigue of superplastic materials, it was hypothesized some years ago [30] that cyclic deformation by intergranular creep should lead to little or no microstructural damage. This hypothesis is largely confirmed by data like that shown in Fig. 20 [31] which compares the shear fatigue behavior of 63Sn-37Pb solder joints in two microstructures: a normal eutectic microstructure, and a refined microstructure made by rapid solidification. When the joints are tested at strain rates that lie primarily within the intergranular creep regime, the fatigue life of the joint with a fine-grained microstructure is greater by at least three times. The generality of this result is indicated by the data shown in Fig. 21 [31], which compares the shear fatigue behavior of a Sn-Bi eutectic joint, which solidified in a normal eutectic microstructure, to that of a geometrically identical 40In-40Sn-20Pb joint that solidified in a fine-grained structure with superplastic behavior. Again, the fatigue life of the superplastic material is greater by a factor of 3 or more.

The utility of these data lies largely in the fact that many small solder joints either develop fine-grained microstructures as a natural consequence of their manufacture or can be made to do so by increasing the rate of cooling during solidification. Intergranular

creep almost certainly contributes to the fatigue life of many existing solder joints, and may help to explain the observation that small Sn-Pb solder joints in electronic devices seem to have better fatigue resistance than design tests on bulk solder would suggest. On the other hand, this technique is not obviously applicable to thicker solder joints, which solidify at slower rates, and may be compromised by grain growth in service, particularly if the joint is subject to long hold times at high homologous temperatures.

The second approach to improving the fatigue life is the use of compositional changes to create an irregular microstructure that resists the formation of planar shear bands. Two methods have been successfully used. First, one may simply adjust the solder composition to an off-eutectic value that produces a mixed microstructure that contains relative large pro-eutectic grains (for example, Fig. 7). In a bimodal microstructure of this sort each constituent disrupts the normal deformation pattern of the other. It has been known for some time that off-eutectic Sn-Pb solders have better fatigue resistance than eutectic material [32-35]. Recent research has documented the mechanistic connection between the improvement in fatigue life and the change in the pattern of deformation[36]. Second, one may use chemical additives to disrupt the formation of the eutectic microstructure, which accomplishes essentially the same effect. In prior research in this laboratory, small additions of In and Cd to 63Sn-37Pb were shown to produce a significant improvement in shear fatigue life. Metallographic analysis shows that they inhibit the completion of the eutectic microstructure, leading to a structure that has broad, featureless bands along the eutectic colony boundaries[10].

The third approach is to introduce dispersants into the solder to disrupt the deformation pattern. Research along these lines is underway in several laboratories. While the research is certainly worthwhile, the approach is problematical. Assuming that a suitably dense distribution of dispersants can be successfully introduced, the fatigue properties of the solder will reflect the constraints on deformation that are imposed by the hard dispersants as well as the benefit from dispersing the matrix slip. In one study recently completed in this laboratory we used the fact that the addition of Au to 63Sn-37Pb solder naturally produce a dense distribution of dispersants (Fig. 22)[37] to explore its consequences for the fatigue life. While small Au additions do seem to improve the fatigue life, these do not produce dense dispersant fields. When the Au addition is sufficient to produce dispersants, as in Fig. 22, the fatigue resistance is lowered rather than raised[37]. At least in this case, the deleterious influence of the distribution of hard precipitates apparently outweighs any benefit from the dispersion of slip in the solder.

Thermal fatigue in shear

The basic mechanisms of shear fatigue are the same whether the temperature is held constant or cycled to generate thermal fatigue like that encountered in service. However, the temperature cycle does produce noticeable differences in the deformation pattern. The shear bands are more coarse in samples subjected to thermal fatigue, and the material within them appears to coarsen more rapidly. A likely source of this difference is the asymmetry of the deformation that is produced by the thermal cycle. When the temperature is increased, the creep rate increases exponentially, with the consequence that

deformation is much easier in the high-temperature phase of the thermal cycle than it is in the low-temperature phase. The sample effectively softens during deformation in the direction of increasing temperature, and hardens during its reverse deformation as the sample cools. As a consequence, the forward and reverse deformation paths will not ordinarily be exactly the same, and the deformation pattern should be more diffuse. Finite element analysis [38] has shown that the thermal strains can lead to irreversibilities that produce a progressive macroscopic deformation of the body of the solder. The increased coarsening observed in thermal fatigue has a similar explanation. Microstructural defects that are preferentially stored in the material during the low-temperature step provide an additional driving force for microstructural change during the high-temperature step where grain growth is relatively easy.

Fatigue in tension

Research on the tensile fatigue of solders has also revealed interesting microstructural effects. For example, tensile fatigue studies on model solder joints of eutectic Sn-Pb solder uncovered a tendency for these joints to fail within the intermetallic layer [21]. This result is consistent with the results of tensile tests that will be reviewed below. It is presumably due to a combination of continuum and microstructural effects. Since the solder joint is thin in the direction of the applied load, the solder has a relatively high effective yield strength, which transfers the load to the intermetallic. The intermetallic is brittle, and hence provides relatively easy propagation paths for fatigue cracks that nucleate at or near the interface. A second interesting result was obtained from cyclic tension tests on bulk specimens of Pb-rich solders [23]. These have microstructures that are made up of relatively equiaxed grains of Pb-rich phase. When they are tested in air under small cyclic loads, they tend to fail by intergranular fracture. The intergranular fracture mode is believed to be promoted by oxygen adsorption on grain boundaries. It should, hence, be inhibited by grain refinement, which creates a more tortuous intergranular path, or by the addition of chemical species that act to getter oxygen.

Deformation and fracture

Since a solder joint must resist loads that are applied during manufacture and transport, its mechanical response to relatively large mechanical loads that are applied at strain rates like those used in ordinary tensile tests are also of interest. However, since solders are ordinarily used and tested at high homologous temperatures, their response is affected by the same microstructural mechanisms that govern creep at high stresses. The deformation of solder joints is particularly sensitive to the geometry of the load, and they behave differently in tension and in shear.

When solder joints are strained to failure in shear the deformation is primarily within the solder. Assuming a high homologous temperature, the joint yields under very low load, hardens to an ultimate tensile strength, and then softens dramatically with further strain. As an example, Fig. 23 shows shear stress-strain curves for a model joint of eutectic Sn-In on Cu at several different temperatures [3]. In this case, strain softening

appears to be due to progressive heterogeneity in the deformation pattern. The solder becomes weaker because less and less of its volume participates in the strain. Eutectic Sn-Pb shows a generally similar behavior, but in this case the strain softening is enhanced by dynamic recrystallization, which not only provides an effective mechanism of recovery, but leads to a microstructure that is considerably softer than the eutectic one.

Soft solders have similar behavior in tensile tests, but strain softening is less pronounced, which reflects the more homogeneous deformation of the specimens. The most striking microstructural influence on the tensile behavior is the aging of the solder microstructure. Tensile properties vary with time. Eutectic Sn-Pb softens noticeably for several months after casting, and continues to change, though at a slower rate, for the life of the specimen. These changes are associated with normal reconfigurations of the microstructure. These occur at a measurable rate at room temperature, which is a relatively high homologous temperature for the alloy. The changes involve precipitation of Sn within the Pb-rich phase, grain growth, and reconfiguration from the eutectic structure toward a more equiaxed arrangement of grains.

When solder joints are tested to failure in tension the ultimate fracture may occur either within the body of the solder or in the intermetallic layer at the interface. The site of the failure depends on the strength of the solder, the nature and thickness of the intermetallic, and the microstructure of the solder. Since the intermetallic is normally brittle, the overall tensile strength of the joint is higher and more nearly reproducible if the microstructure is changed to promote fracture through the solder bulk.

These principles are illustrated by tensile tests on 60Sn-40Pb and 95Pb-5Sn solder joints on copper [39]. The 95Pb-5Sn solder is the weaker of the two. In the as-solidified condition, it fractures within the solder through void nucleation at Sn-rich precipitates in the Pb-rich grains. When the joint is reflowed to thicken the Cu_3Sn intermetallic layer at the interface, Sn is depleted from the matrix. The fracture site shifts to the solder-Cu interface, and the fracture strength decreases by more than 50%.

The behavior of eutectic 60Sn-40Pb on Cu is quite different. When it is solidified at slow to moderate rates, this solder has a basically eutectic microstructure with a double-layer of intermetallic at the interface (Cu_6Sn_5 on Cu_3Sn, as in Fig. 8). In this case the solder fails through the Cu_6Sn_5 intermetallic layer. The apparent reason is the greater strength of the solder, which increased the load on the intermetallic. Reflow treatments that increase the thickness of the intermetallic cause a significant decrease in strength, with the same fracture mode. Small changes in the composition of the solder that do not change the fracture mode have almost no effect on the joint strength. However, if the solidification pattern of the joint is such that long rods of Cu_6Sn_5 intermetallic are released into the body of the solder, as in Fig. 24 [40], these may serve as void nucleation sites that shift the fracture from the interface into the solder. When this happens, the ductility of the solder has the consequence that the tensile strength increases slightly.

These results suggest the importance of maintaining a thin intermetallic layer to preserve the tensile strength of the solder joint. They also show that inclusions (or, by ex-

tension, small voids) in the solder are not necessarily sources of weakness. They may act to preserve strength by ensuring that the crack path runs through the solder.

A final interesting fracture behavior is observed when eutectic Sn-Pb solder joints on Cu are fractured in liquid nitrogen. The fracture path runs along the solder-Cu_6Sn_5 interface, as shown in Fig. 25 [39], even though this interface is irregular and leads to a tortuous fracture path. The appearance of the fracture surface suggests that the Pb-rich phase remains well bonded to the intermetallic even at 77K; islands of Pb-rich material adhere to the intermetallic. The source of this curious fracture mode seems to be the debonding of Sn. The probable reason for this behavior is the anisotropic thermal contraction of metallic Sn, which has a complex, tetragonal crystal structure. This thermal contraction produces strains at the interface with the rigid intermetallic, causing the two to separate cleanly.

Conclusion

The examples given above should suffice to show that the microstructure of a solder joint cannot be ignored if its mechanical properties are to be understood. Changes in the microstructure can, and do cause dramatic changes in mechanical properties and failure modes.

On the other hand, the current state of materials science does not offer the level of theoretical guidance that is needed to construct microstructure-based mechanical models. It appears that for the foreseeable future these will have to be based on fairly straightforward constitutive relations.

While the metallurgy does not provide an accurate theory, it does provide scientific guidance that ought to be useful to those who must construct predictive models. Given the microstructural complexity of solder behavior, the constitutive equations used in these models should be taken from tests on solder joint configurations that bear the closest possible microstructural resemblance to those that are addressed by the model, and are subject to load geometries that resemble the loads of interest. It is incorrect, and may be badly misleading, to adopt a constitutive relation simply because it was measured on a material that has a particular chemical composition.

Similar considerations pertain to the design of accelerated tests that are used to confirm or refine predictive models. An accelerated test is probative to the extent that is accelerates the mechanism that governs the behavior of interest. If the method of acceleration changes the microstructure or the microstructural mechanisms that operate, the test may mislead rather than inform. For example, accelerating creep by increasing the applied stress may change the basic mechanism of creep unless one is careful; accelerating creep by increasing the temperature may trigger microstructural changes that have the same undesirable effect.

ACKNOWLEDGMENT

REFERENCES

[1] J.L. Freer Goldstein and J.W. Morris, Jr., submitted to *Metall. Trans. A.*

[2] Z. Mei, M.C. Shine and J.W. Morris, Jr., *ASME Journal of Electronic Packaging,* **113**, 109 (1991).

[3] J.L. Freer Goldstein and J.W. Morris, Jr., unpublished work.

[4] D.R. Frear, J.B. Posthill, and J.W. Morris, Jr., *Metallurgical Transactions A*, **20A**, 1325 (1989).

[5] Z. Mei and J.W. Morris, Jr., *J. Electronic Mater.*, **20**, 599 (1991).

[6] T.S.E. Summers, Ph.D. Thesis, University of California at Berkeley, May 1991.

[7] A.J Sunwoo, J.W. Morris, Jr., and G.K. Lucey, Jr., *Metall. Trans. A*, **23A**, 1323 (1992).

[8] Z. Mei, A.J. Sunwoo, and J.W. Morris, Jr., *Metall. Trans. A*, **23A**, 857 (1992).

[9] D. Grivas, D. Frear, L. Quan, and J.W. Morris, Jr., *J. Electronic Mater.*, **15**, 355 (1986).

[10] D. Tribula, Ph.D. Thesis, University of California at Berkeley, June 1990; and D. Tribula and J. W. Morris, Jr., *ASME Journal of Electronic Packaging*, **112**, 87 (1990)

[11] P.A. Kramer, M.S. Thesis, University of California at Berkeley, May 1992.

[12] Z. Mei and J.W. Morris, Jr., *J. Electronic Mater.*, **21**, 599 (1992).

[13] Bird, J.E., A.J. Mukherjee, and J.F. Dorn, *Quantitative Relation Between Properties and Microstructure*, 255 (Israel University Press, 1969).

[14] P.A. Kramer, J. Glazer, and J.W. Morris, Jr., submitted to *Metall. Trans. A*

[15] D. Grivas, M.S. Thesis, University of California at Berkeley, Jan. 1974.

[16] Z. Mei, D. Grivas, M.C. Shine and J.W. Morris, Jr., *J. Electronic Mater.*, **19**, 1273 (1990).

[17] Z. Mei and J.W. Morris, Jr., *J. Electronic Mater.*, **21**, 401 (1992).

[18] Tsung-Yu Pan, Ford Motor Company, Third International Workshop on Materials and Mechanics Issues of Solder Alloy Applications, Santa Fe, September, 1993

[19] H.D. Solomon, *J. of Electronic Packaging*, **111**, 75 (1989)

[20] M.C. Shine and L.R. Fox, ASTM STP 942, H.D. Solomon, et al., ed., 1988, p 588.

[21] D. Frear, D. Grivas and J.W. Morris, Jr., *J. Electronic Mater.*, **18**, 671 (1989).

[22]   S. Vaynman, M.E. Fine, D.A. Jeannotte, *Metall. Trans. A*, **19A**, 1051 (1988).

[23]   D. Frear, Ph.D thesis, University of California at Berkeley, 1987.

[24]   K.G. Schmitt-Thomas and S. Wege, *Brazing and Soldering*, **11**, 27 (1986)

[25]   W.M. Wolverton, *Brazing and Soldering*, **12**, 33 (1987)

[26]   J.N. Keller, *IEEE Transactions on Components, Hybrids, and Manufacturing Technology*, 1986, **4**,132 (1986).

[27]   J.T. Lynch, M.R. Ford and A. Boetti, *IEEE Transactions on Components, Hybrids, and Manufacturing Technology*, **6**, 237 (1983)

[28]   R.N. Wild, *Welding Journal (Res. Suppl.)*, **51**, 521 (1972)

[29]   W.L. Winterbottom, private communication.

[30]   J.W. Morris, Jr. and Z. Mei, in <u>Solder Mechanics, A State of the Art Assessment</u>, D.R. Frear, W.B. Jones, K.R. Kinsman eds., TMS 1991.

[31]   Z. Mei and J.W. Morris, Jr., *Trans. ASME, J. Electronic Packaging*, **114**, 104 (1992).

[32]   E.R. Bangs and R.E. Beal, *Welding Journal (Res. Suppl.)*, **54**, 377s (1978).

[33]   H. Inoue, Y. Kurihara, and H. Hachino, *IEEE Transactions on Components, Hybrids, and Manufacturing Technology*, **9**, 190 (1986).

[34]   D.M. Jarboe, Technical Communications Bendix, Kansas City: BDX-613-2341 (1980).

[35]   R.N. Wild, IBM Technical Paper No. 74Z000481, 1975.

[36]   T.S.E. Summers and J.W. Morris, Jr., *Trans. ASME, J. Electronic Packaging*, **112**, 94 (1990).

[37]   P.A. Kramer, Z. Mei, and J.W. Morris, Jr., unpublished work.

[38]   Fuh-Kuo Chen, Ph.D. Thesis, University of California at Berkeley, 1989.

[39]   L. Quan, D. Frear, D. Grivas, J.W. Morris, Jr., *J. Electronic Mater.*, **16**, 203 (1987).

[40]   D. Frear, D. Grivas, and J.W. Morris, Jr., *J. Electronic Mater.*, **16**, 181 (1987).

LIST OF FIGURES

Figure 17: Optical micrographs of a deformed Sn-Pb solder joint. The top micrograph shows the surface relief, which is concentrated in a narrow band along the bottom of the joint. The bottom micrograph, the same region after light polish, shows the band of coarsened and recrystallized material which developed in the highly deformed region.

Figure 18: Creep data for eutectic Sn-Pb, showing (a) transition from dislocation climb-controlled creep to grain boundary-controlled creep, and (b) transition from grain boundary-controlled creep to dislocation glide-controlled creep.

Figure 19: Series of optical micrographs of 60Sn-40Pb solder joint microstructure as a function of number of cycles in thermal fatigue.

Figure 20: Comparison of isothermal fatigue life for solder joints cooled at various rates, tested at two different temperatures.

Figure 21: Comparison of isothermal fatigue life for five solder alloys.

Figure 22: Optical micrographs of solder joint made from eutectic Sn-Pb plus 2.5 weight percent Au.

Figure 23: Stress-strain curves for eutectic In-Sn on Cu tested at 40 °C and three different strain rates.

Figure 24: Optical micrograph showing Cu_6Sn_5 intermetallics within Sn-Pb joint.

Figure 25: SEM micrograph of 60Sn-40Pb sample on Cu failed in tension.
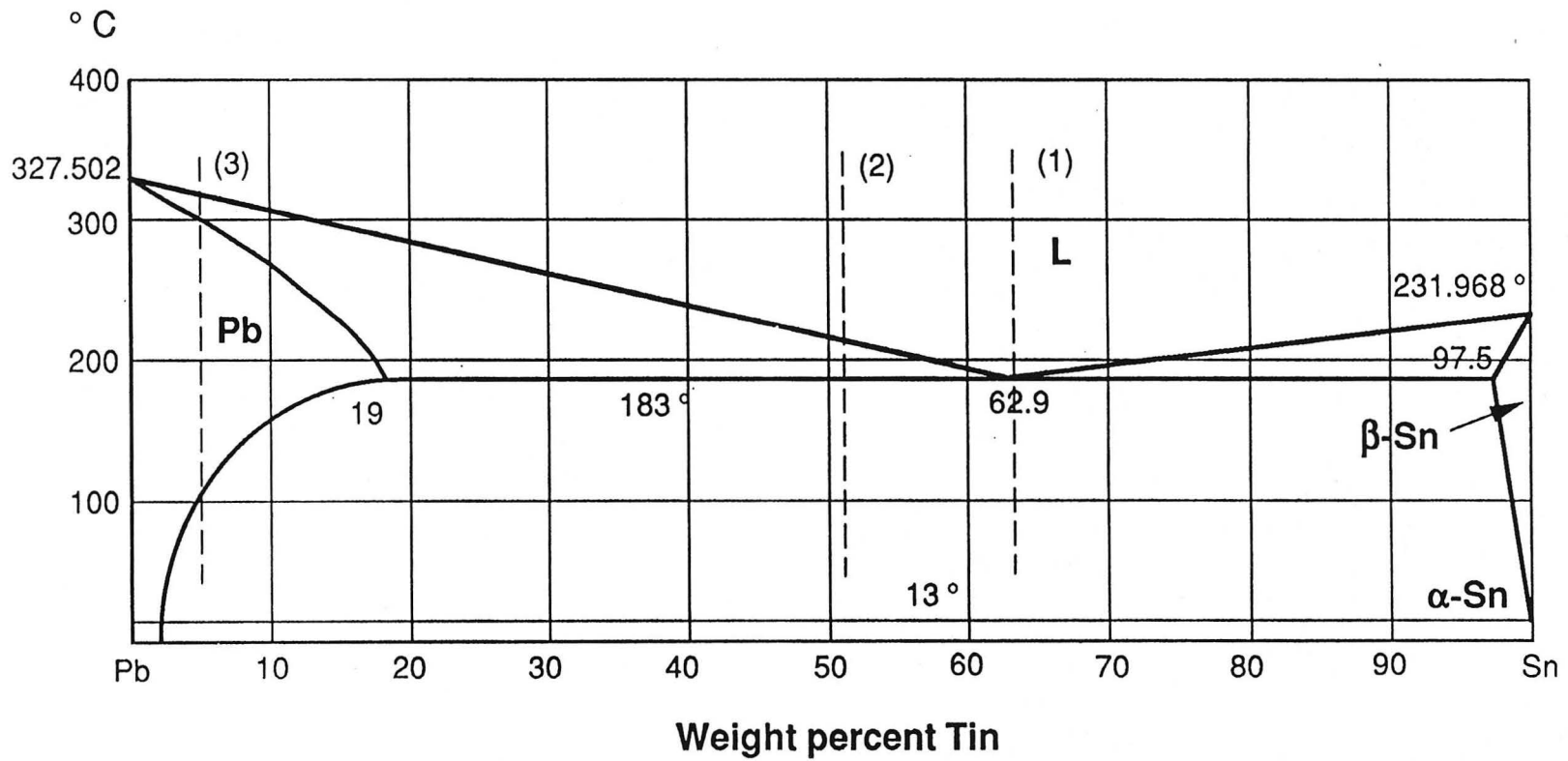
Figure 1: Sn-Pb phase diagram.
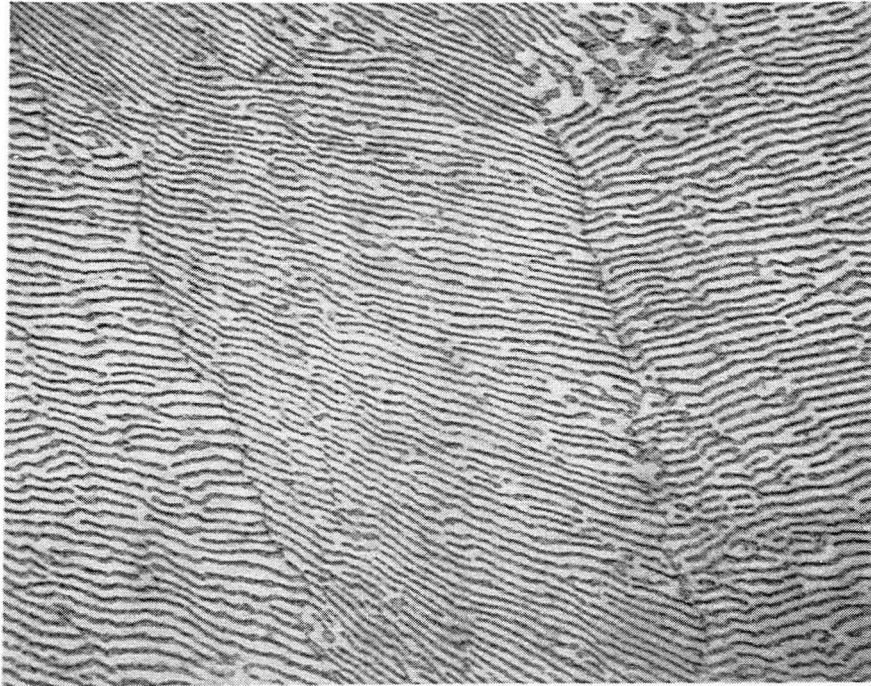
63-37 furnace-cooled ___ 10 μm

Figure 2: Optical micrograph of a eutectic Sn-Pb solder, showing colonies and colony boundaries. XBB 918-6860 (bottom).
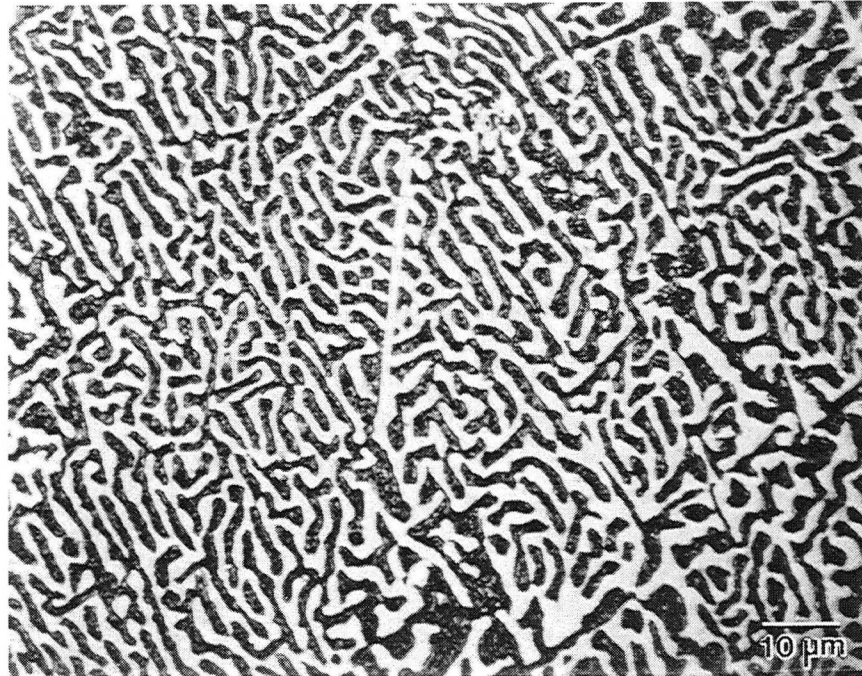
Figure 3:   Optical micrographs of (a) 58Bi-42Sn, a eutectic with similar volume fractions of both phases. XBB 920-9579A. (b) 52In-48Sn, a eutectic in which one phase predominates. XBB 932-622. (c) 96.5Sn-3.5Ag, a eutectic with the major phase comprising over 90 percent by volume. XBB 932-625.

20KU   1.00KX 10.0P 0041
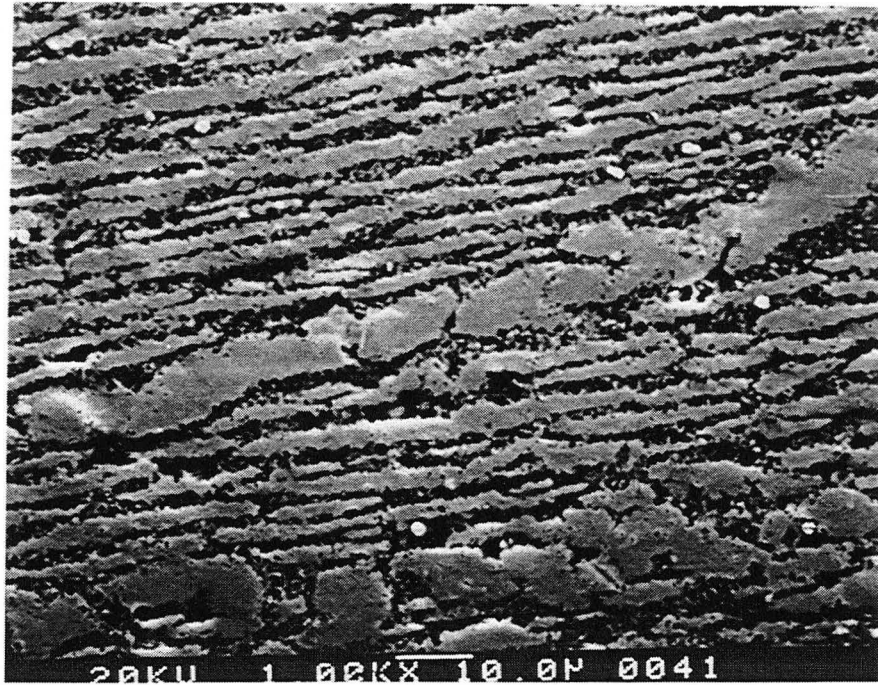
Figure 3 (b)

Figure 3 (c)
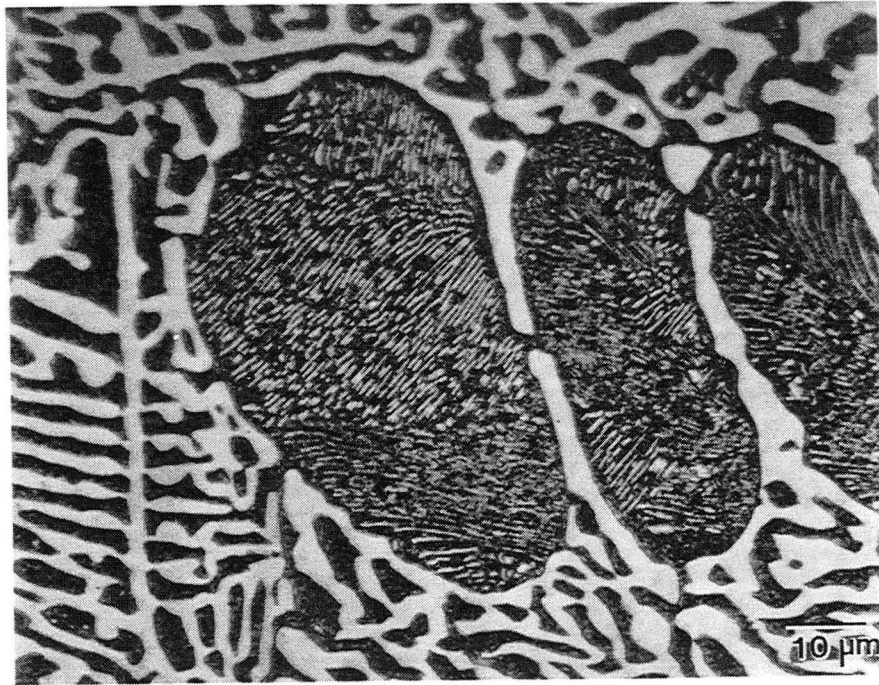
Figure 4:   Optical micrograph of a region of a Bi-Sn eutectic, showing Bi (light)
precipitating within the Sn-rich phase (dark). XBB 932-627.
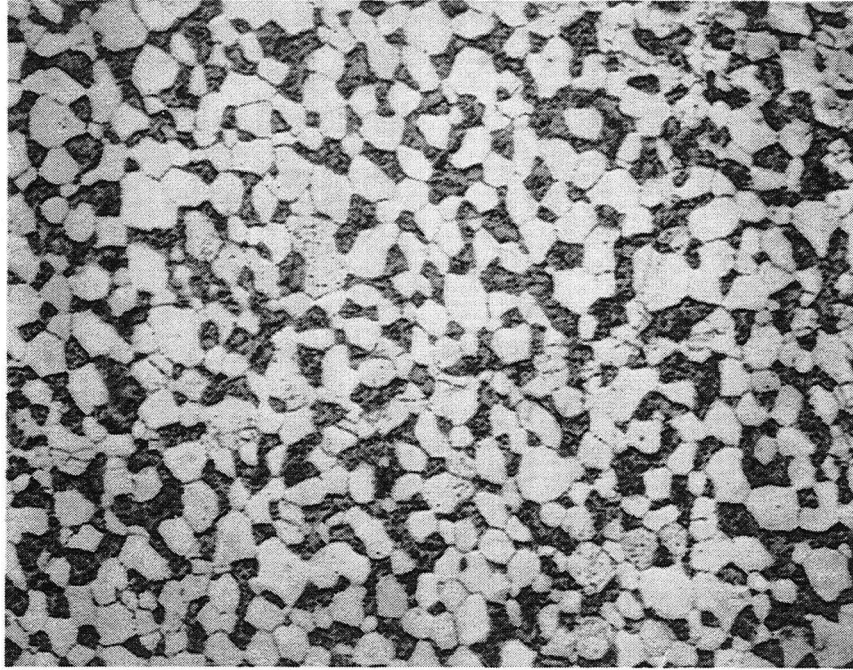
——— 10 μm

Figure 5:   Optical micrograph of a eutectic Sn-Pb solder after cold work and
            recrystallization, showing equiaxed grains. XBB 932-700.
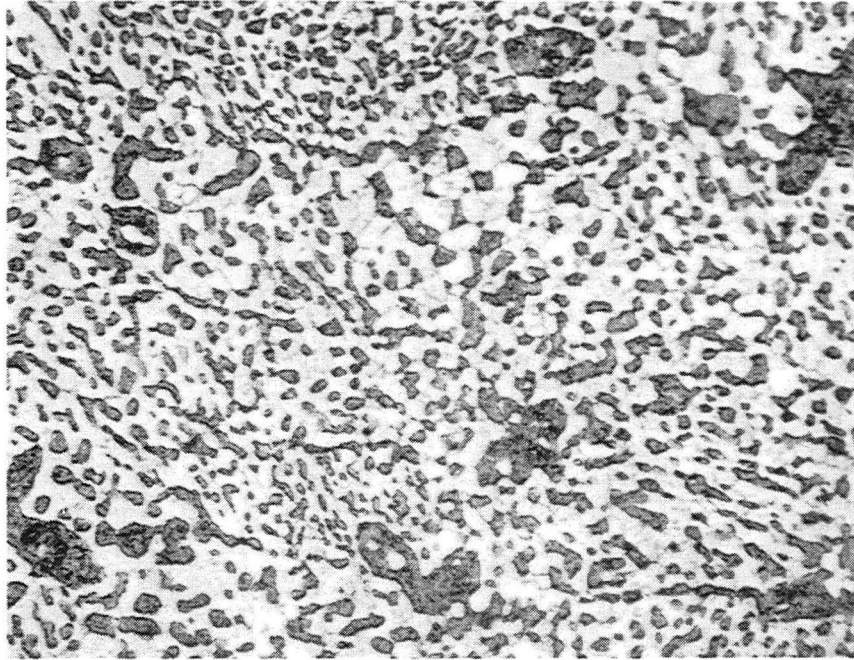
60–40 quenched _____ 10 μm

Figure 6: Optical micrograph of rapidly solidified 60Sn-40Pb, with a primarily equiaxed microstructure. XBB 900-10097 (bottom).
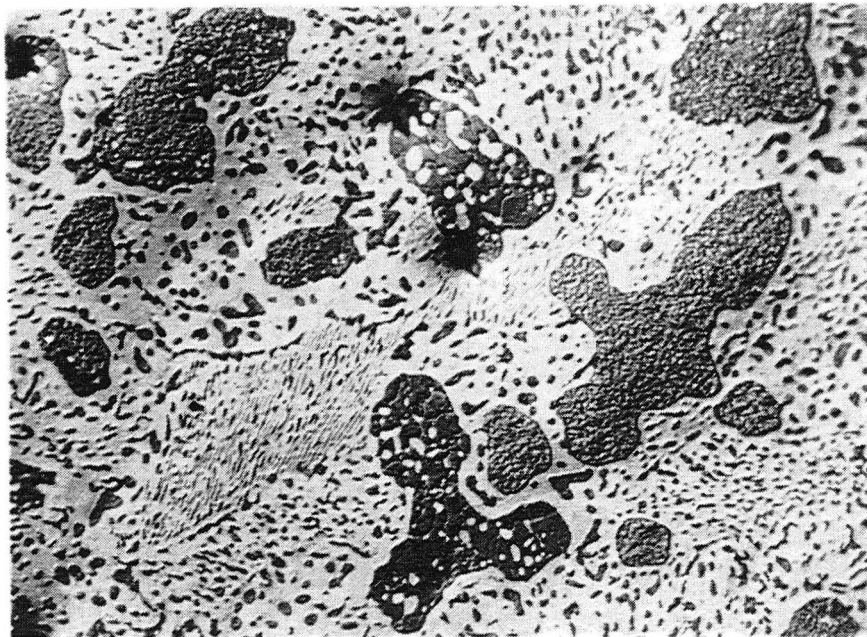
Figure 7:   Optical micrograph of off-eutectic 50Sn-50Pb, with Pb-rich islands in a eutectic matrix. XBB 898-6545C.

0 day   1 day   2 days   4 days

10 μm

9 days   16 days   36 days   54 days
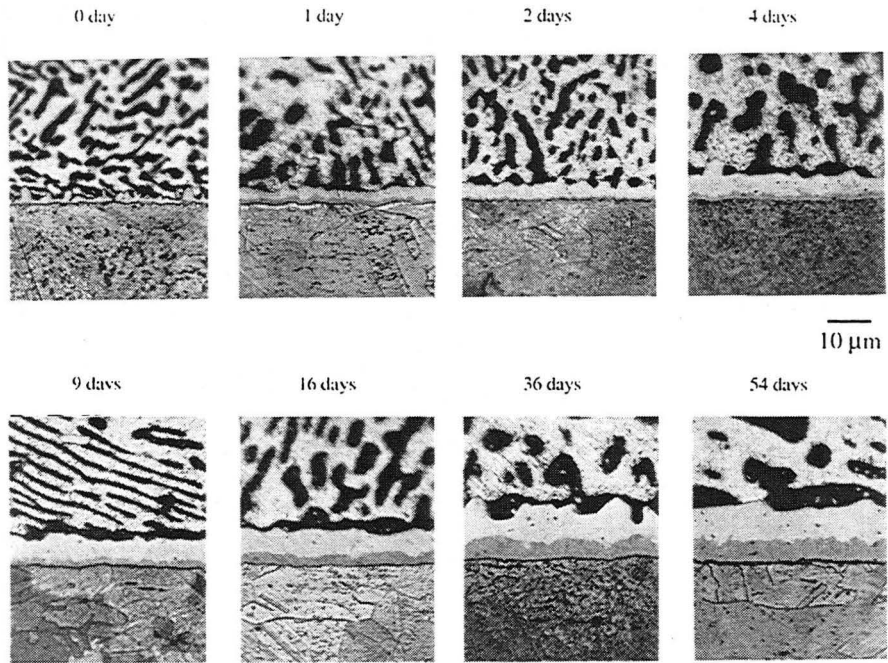
Figure 8:   Series of optical micrographs showing growth of intermetallic layers at the
interface between Sn-Pb solder and copper. There is a layer of Cu_3Sn
(darker) on the copper side and Cu_6Sn_5 on the solder side. XBB 908-6618A.
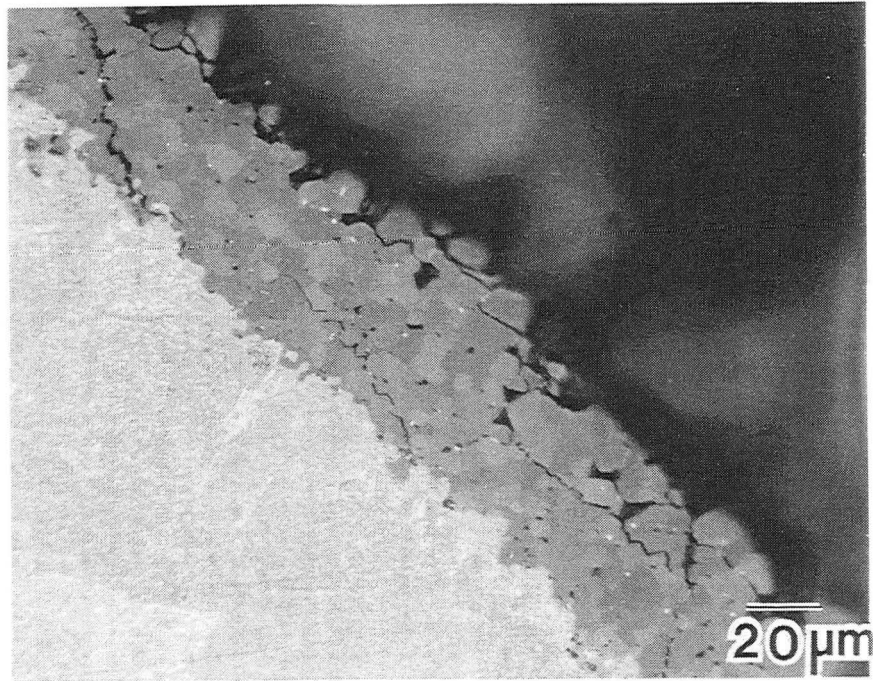
Figure 9: Cu₃Sn layer at the interface between 95Pb-5Sn solder and copper. CBB 854-2607A.
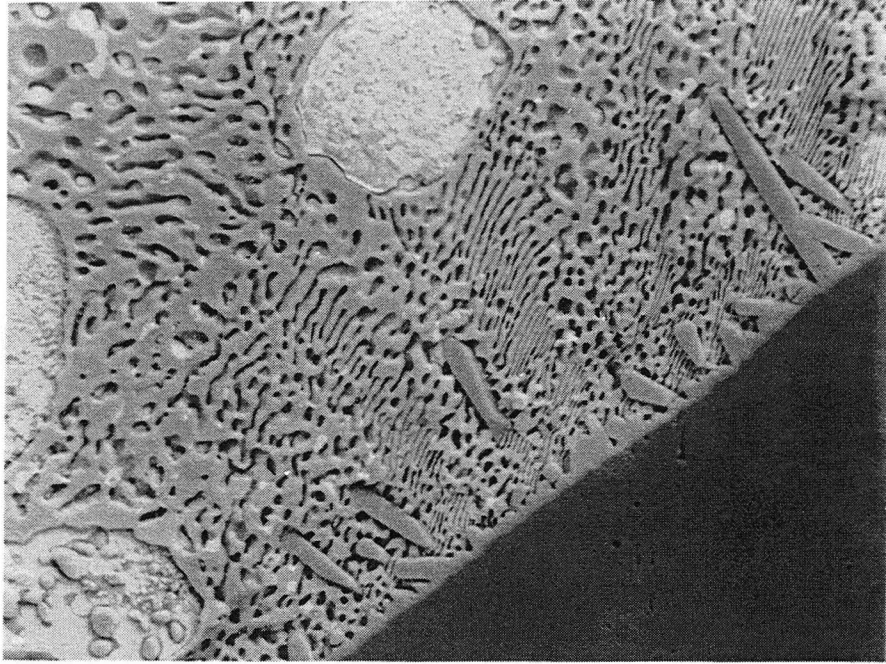
Figure 10: SEM micrograph showing Cu_6Sn_5 intermetallics growing into Sn-Pb solder. XBB 869-7448 (top).
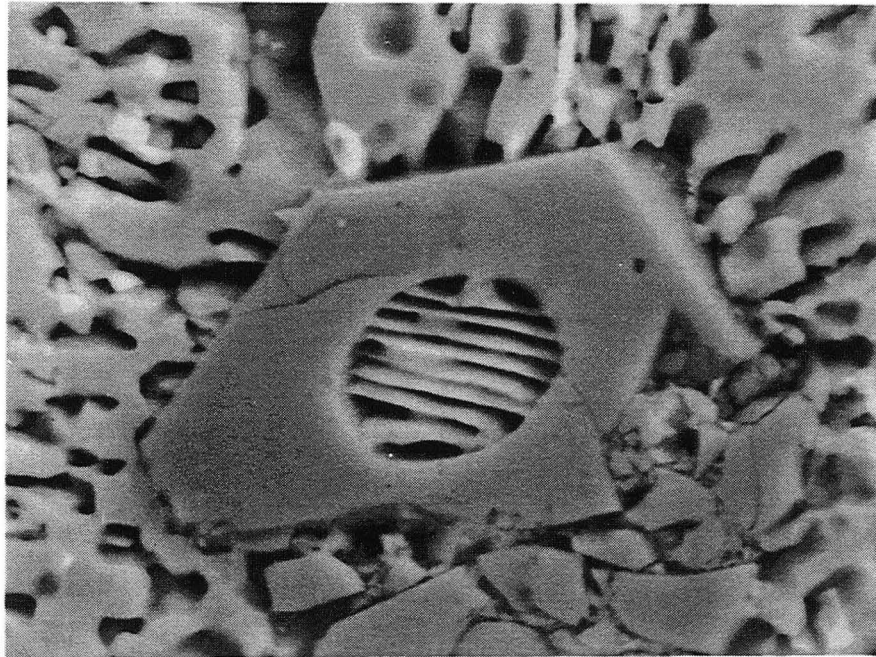
Figure 11: SEM micrograph showing the cross-section of a rod of Cu_6Sn_5 within the Sn-Pb solder joint. It has presumably broken off from the interface during solidification. XBB 869-7448 (bottom).
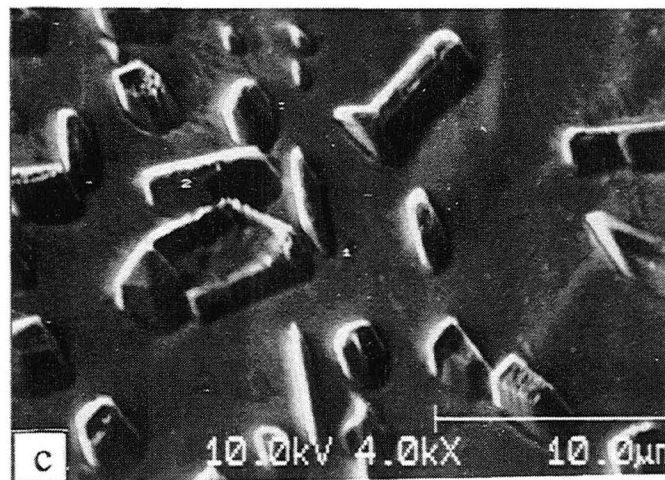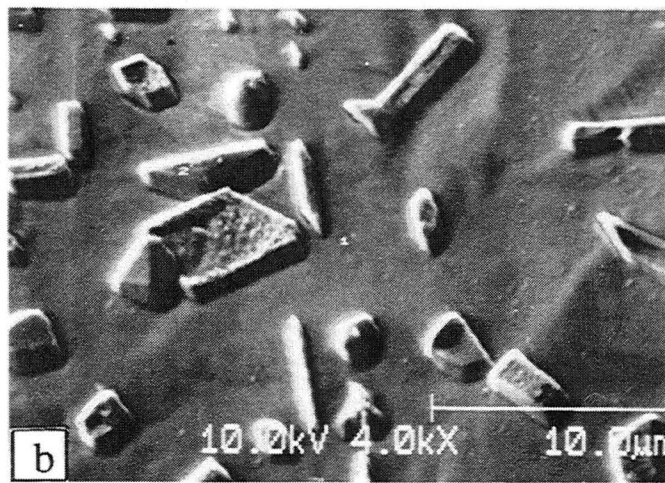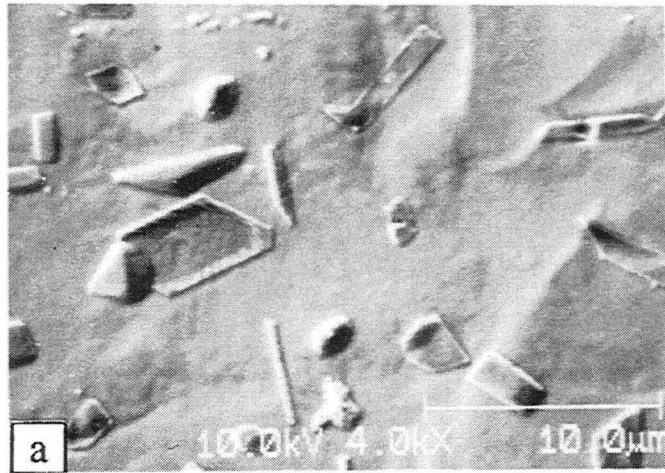
Figure 12: SEM micrographs of the surface of a pre-tinned sample after successively longer sputter times. Intermetallic particles can be seen protruding from the surface of the solder. XBB 900-10279A.
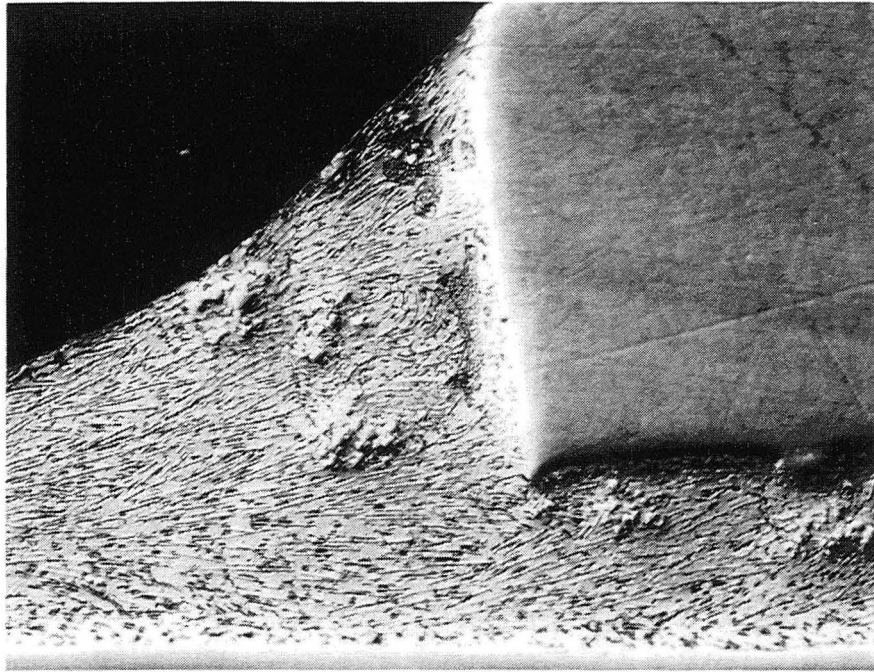
25μm

Figure 13: Optical micrograph of a eutectic Sn-Pb solder joint formed on Au plating, showing the $AuSn_4$ intermetallics which form within the solder. XBB 909-7875.
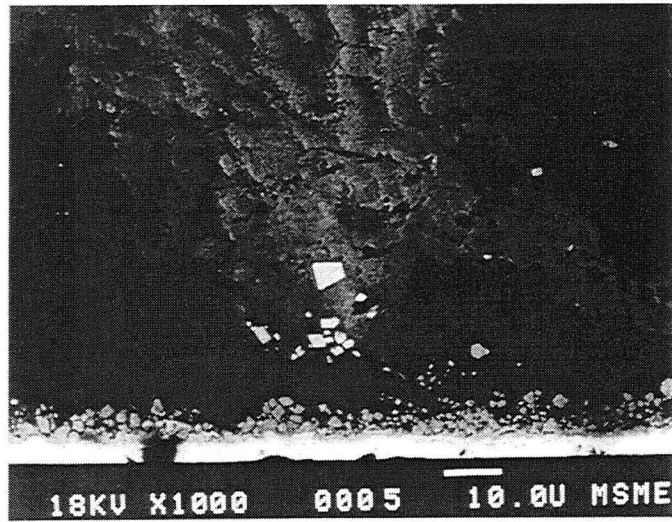
——— 10 μm

Figure 14: Backscattering SEM image of 52In-48Sn solder on Au-coated Cu plate, showing In₂Au intermetallic particles with a layer of undissolved Au underneath (bottom of micrograph). XBB 932-626.
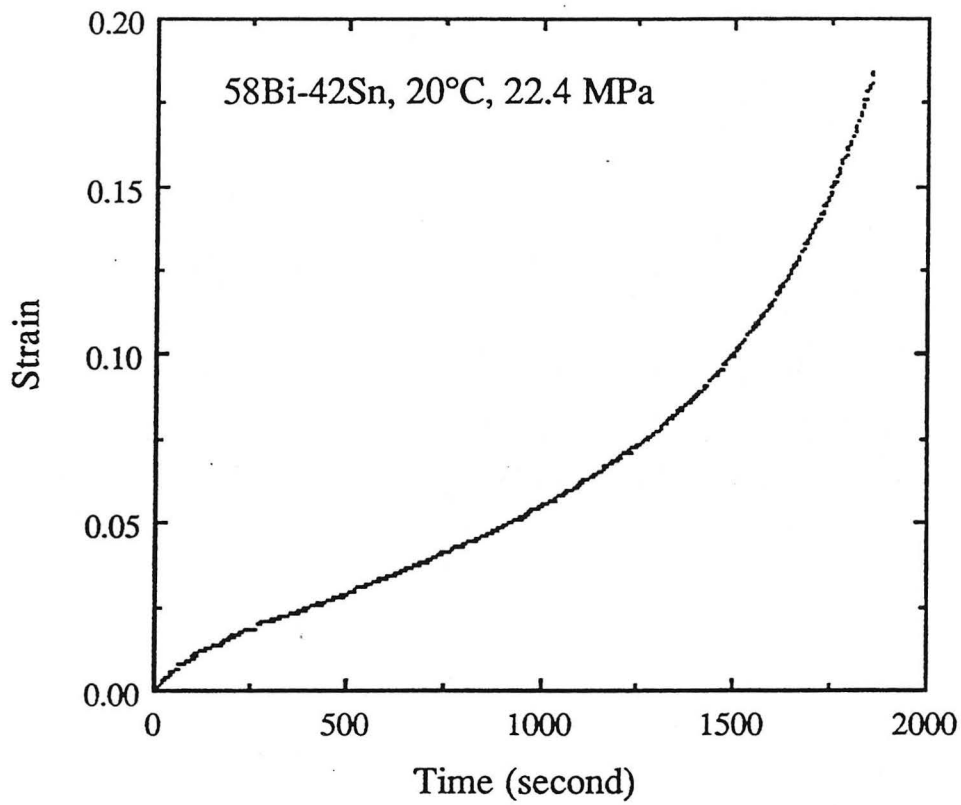
Figure 15: A typical creep curve for a eutectic Bi-Sn solder joint.
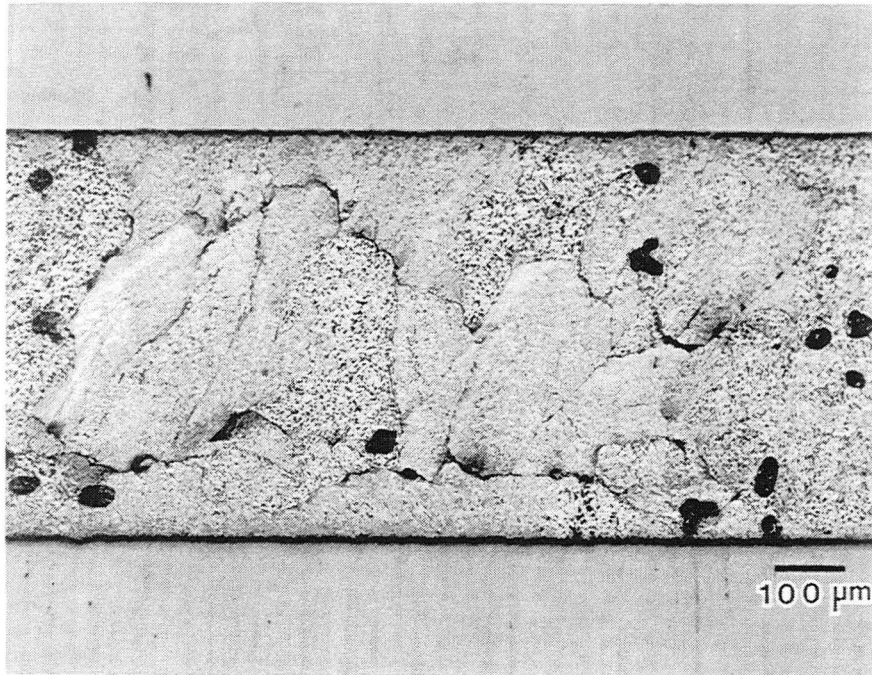
Figure 16: Optical micrograph of deformed 60Sn-40Pb solder joint, showing that the deformation pattern follows microstructural features such as colony boundaries. XBB 902-1232.
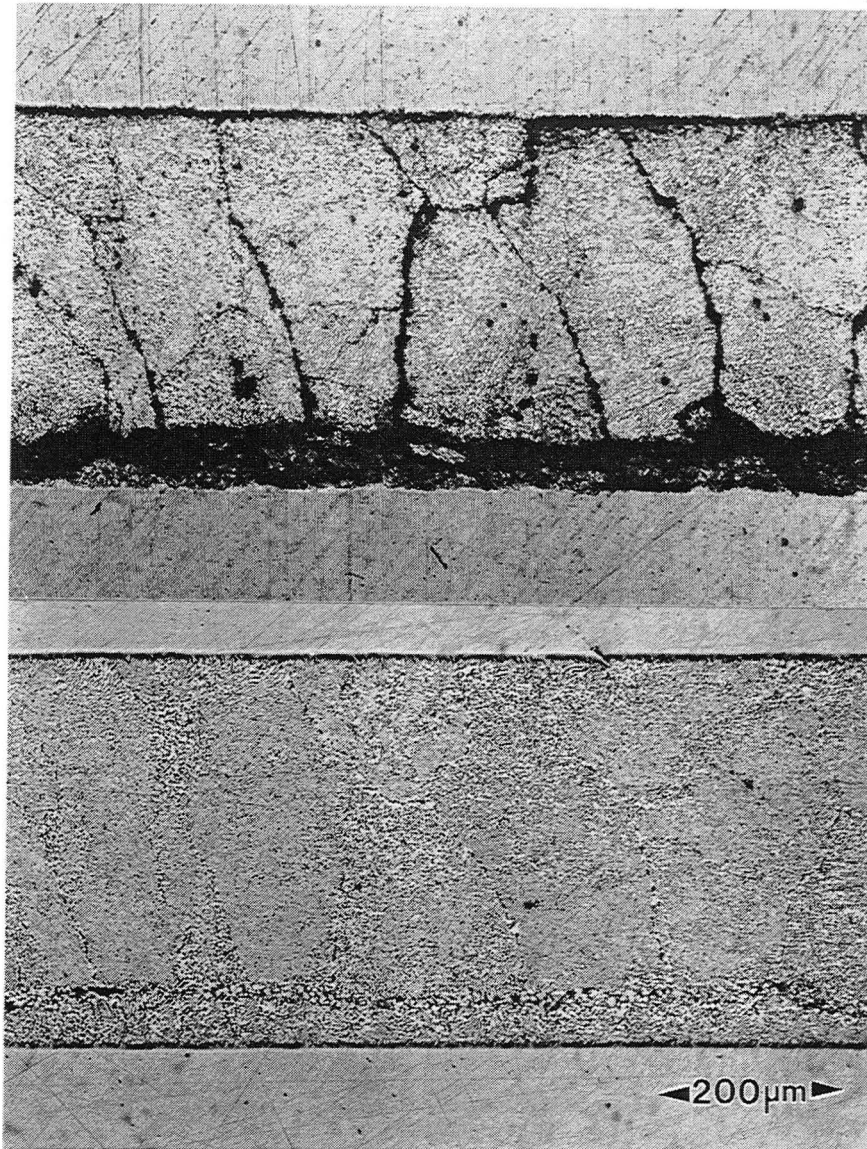
Figure 17: Optical micrographs of a deformed Sn-Pb solder joint. The top micrograph shows the surface relief, which is concentrated in a narrow band along the

bottom of the joint. The bottom micrograph, the same region after light polish, shows the band of coarsened and recrystallized material which developed in the highly deformed region. XBB 887-7084.
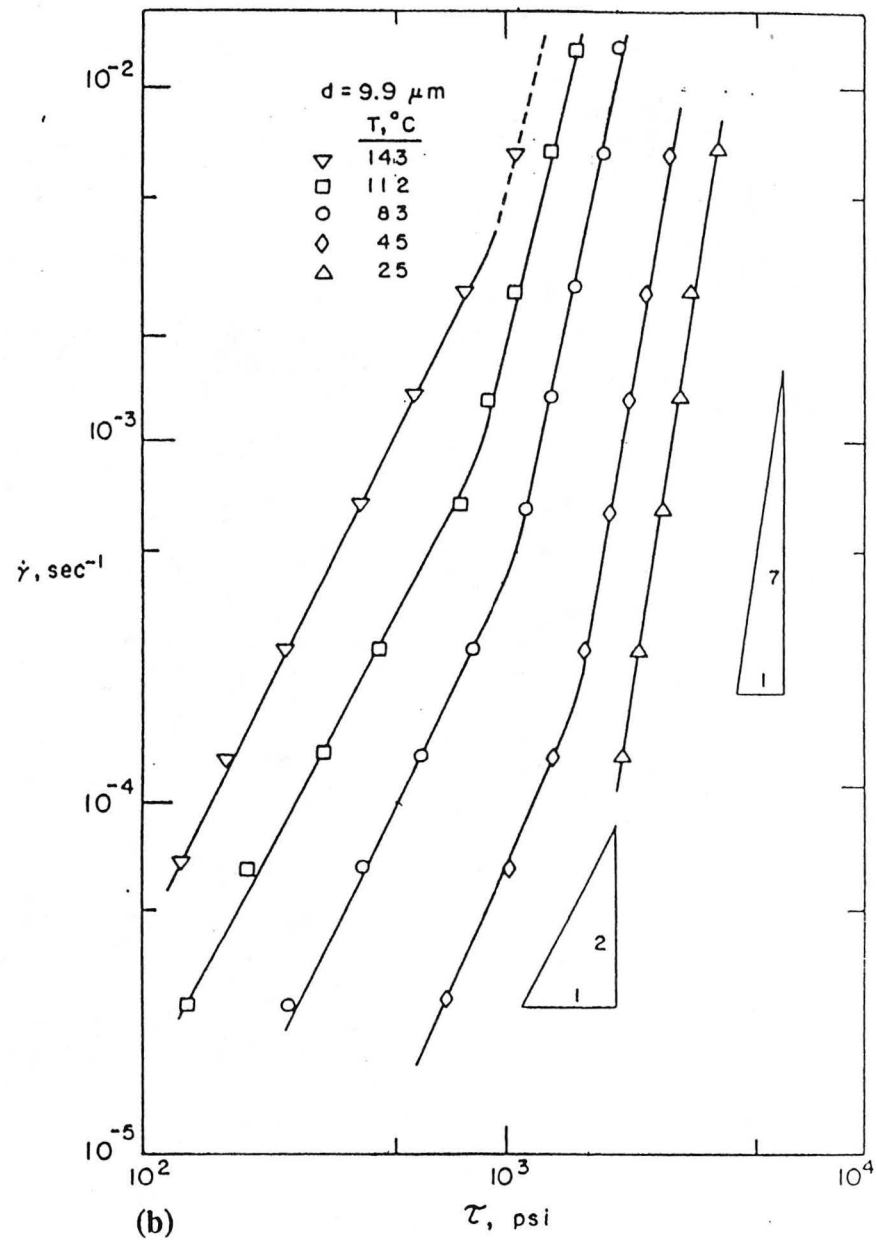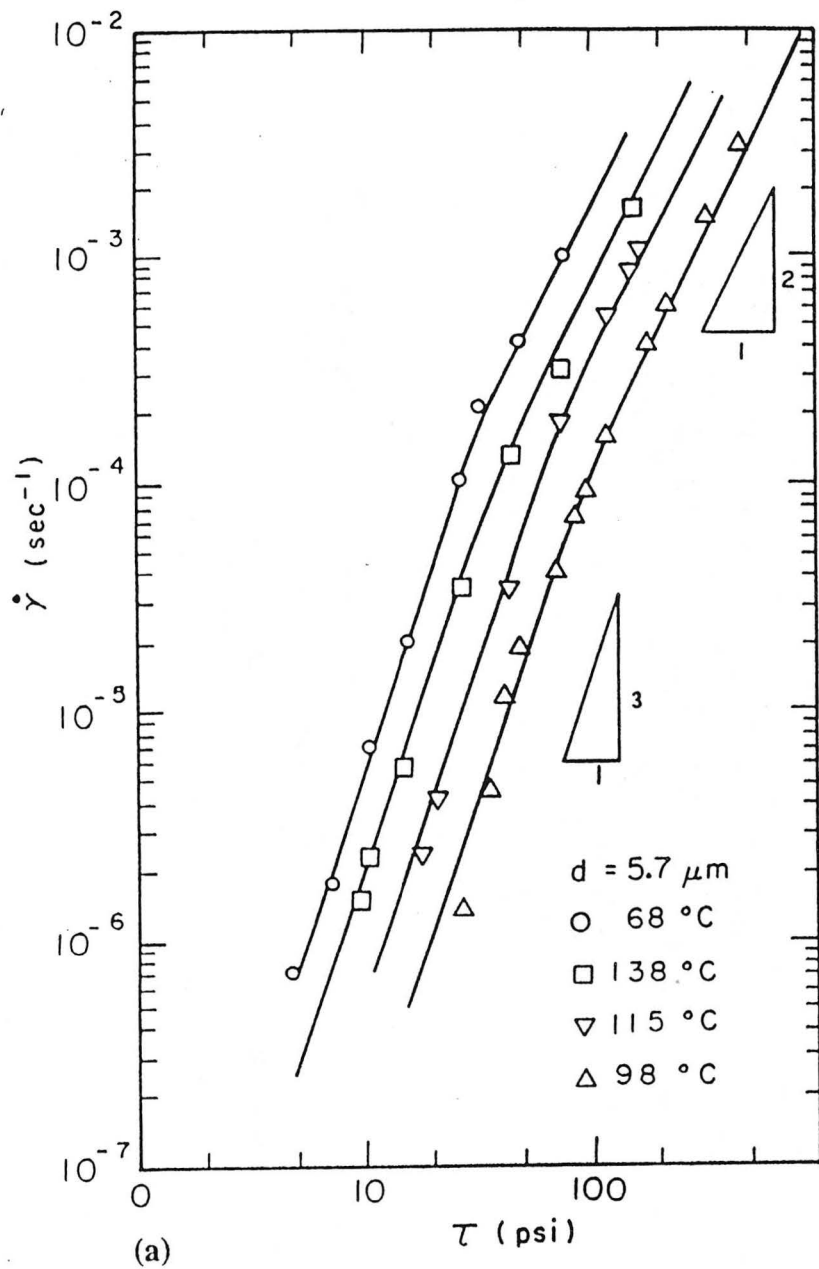
Figure 18: Creep data for eutectic Sn-Pb, showing (a) transition from dislocation climb-controlled creep to grain boundary-controlled creep, and (b) transition from grain boundary-controlled creep to dislocation glide-controlled creep.

60Sn-40Pb
Thermal Cycle: -55°C ←→ 125°C

0 cycles

625 cycles

1000 cycles

1300 cycles

2000 cycles
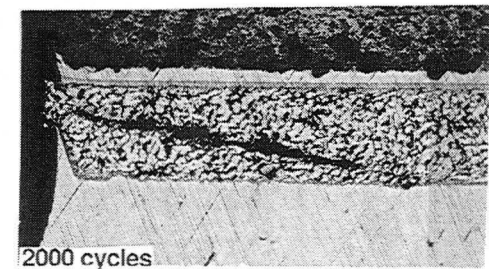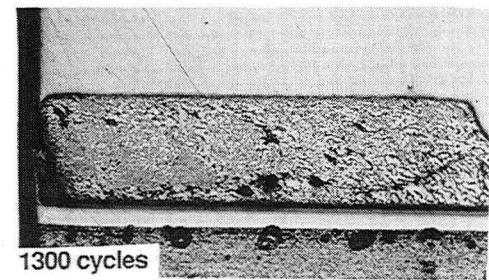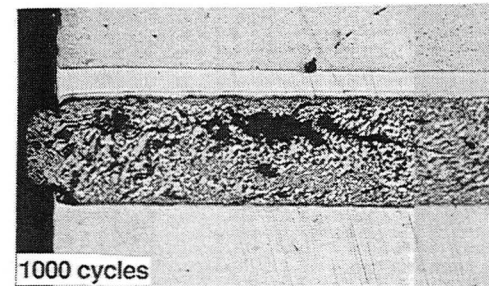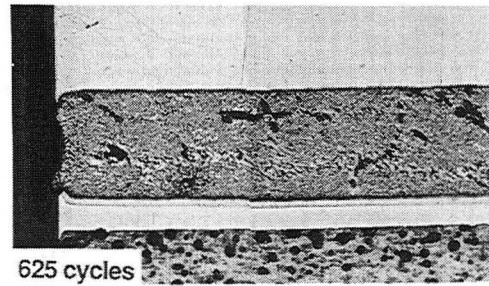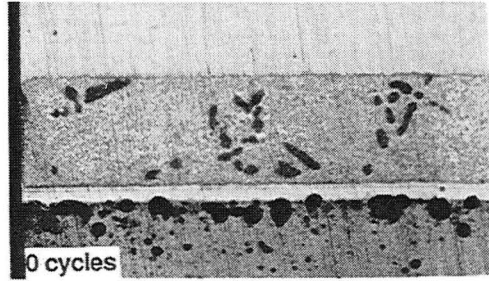
1 mm

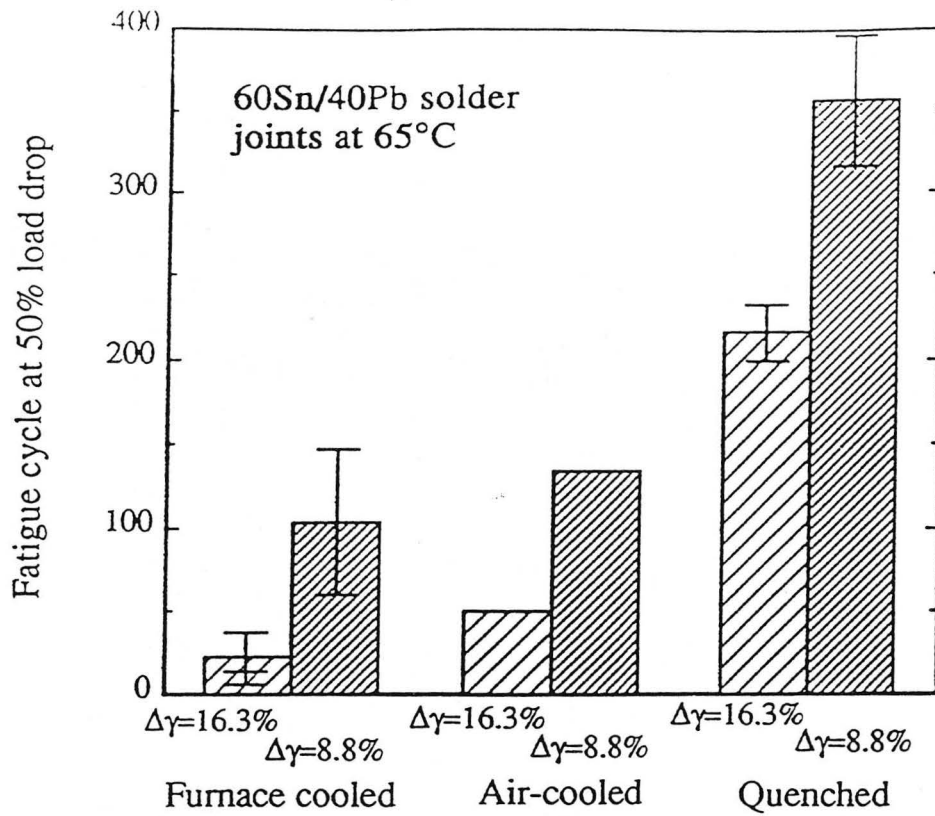Figure 19: Series of optical micrographs of 60Sn-40Pb solder joint microstructure as a function of number of cycles in thermal fatigue. XBB 872-1250.
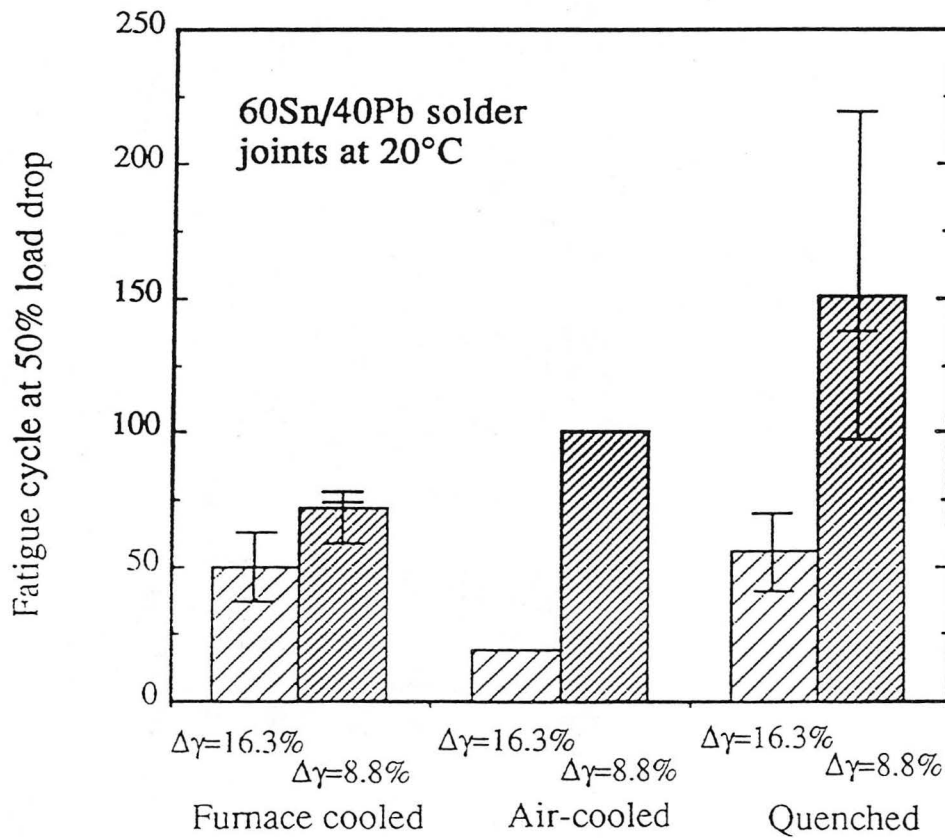
Figure 20: Comparison of isothermal fatigue life for solder joints cooled at various rates, tested at two different temperatures.
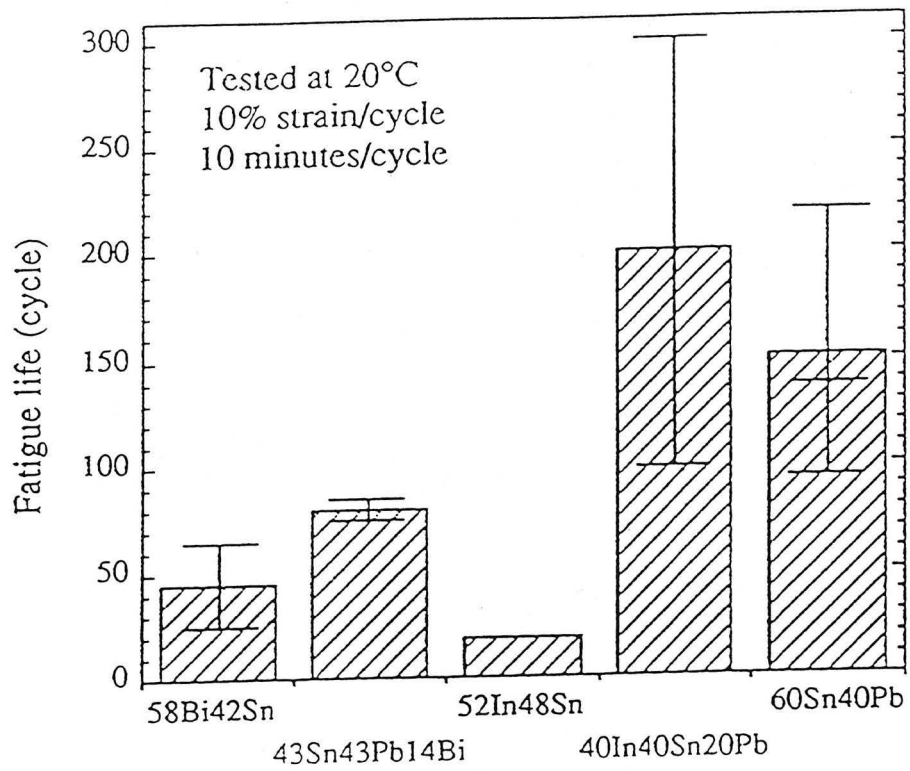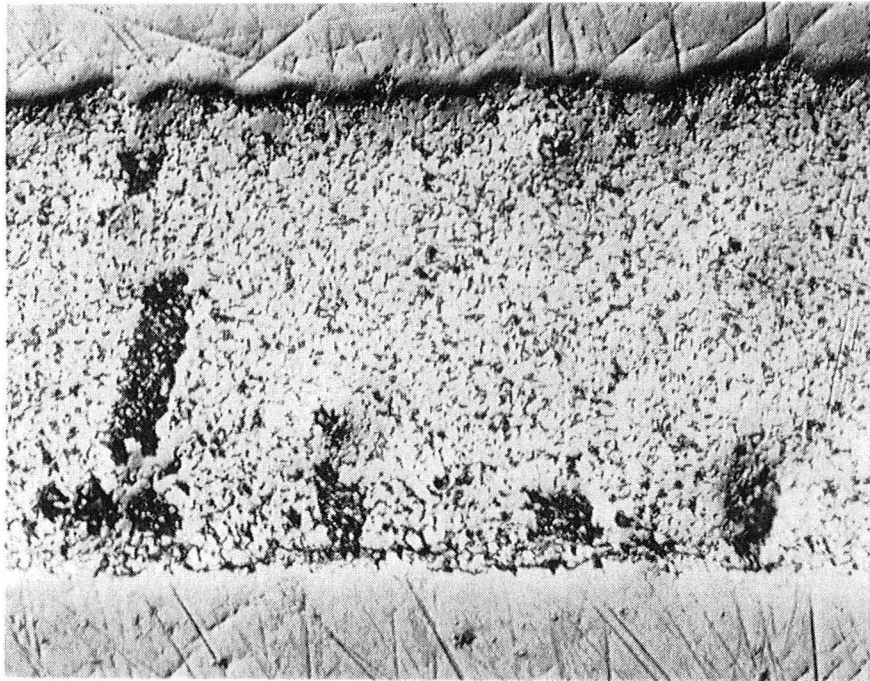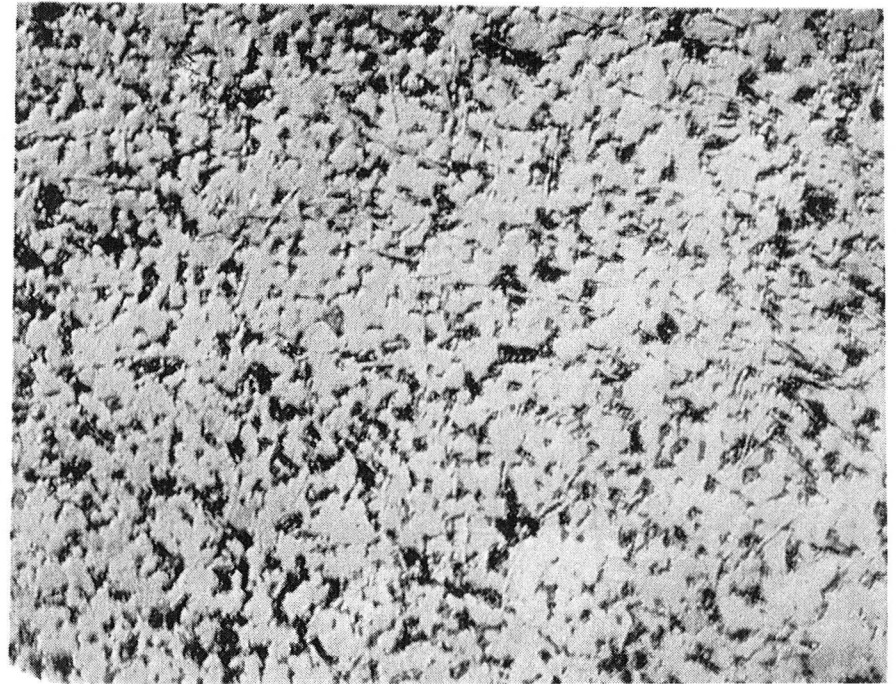
Figure 21: Comparison of isothermal fatigue life for five solder alloys.

$\overline{\text{25}\mu\text{m}}$

$\overline{\text{25}\mu\text{m}}$

Figure 22: Optical micrographs of solder joint made from eutectic Sn-Pb plus 2.5 weight percent Au. XBB 932-716.
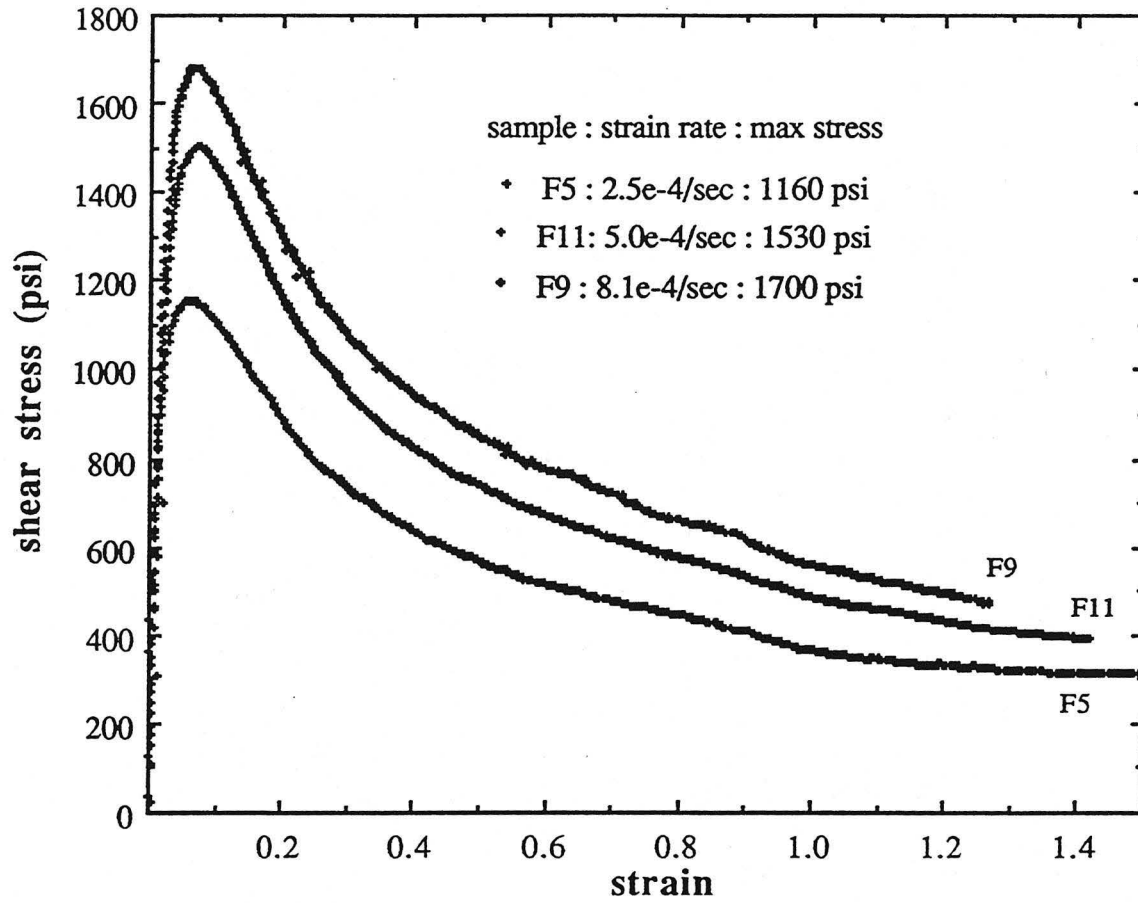
Figure 23:   Stress-strain curves for eutectic In-Sn on Cu tested at 40 °C and three
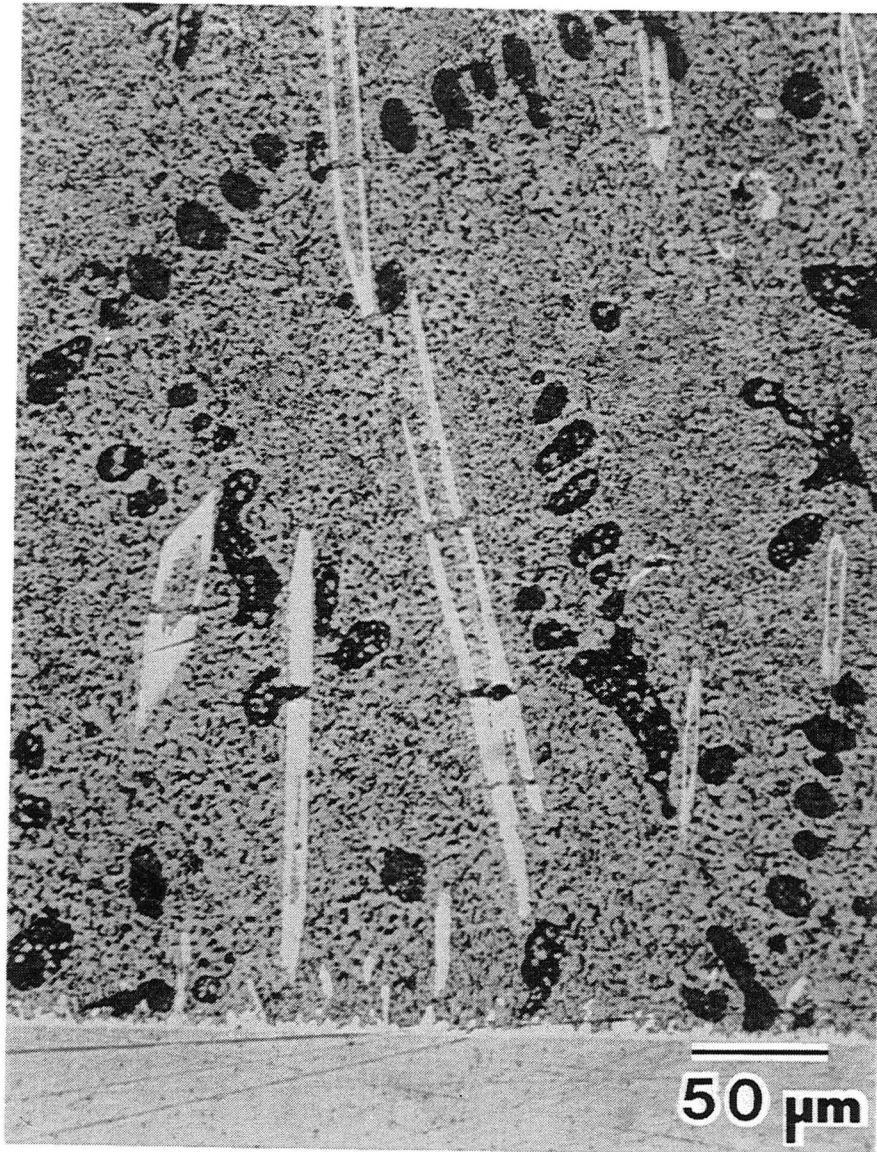   different strain rates.

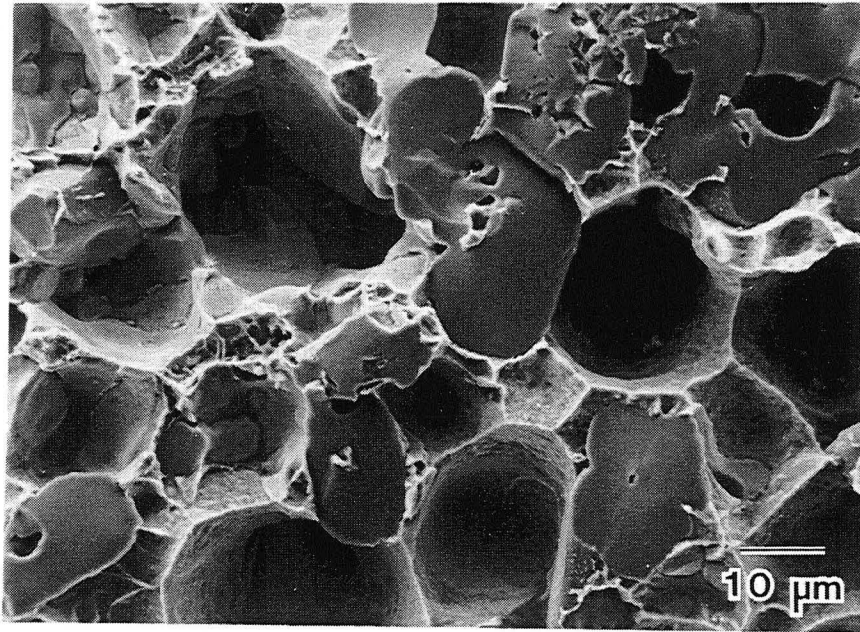Figure 24: Optical micrograph showing Cu_6Sn_5 intermetallics within Sn-Pb joint. XBB 871-422.

Figure 25: SEM micrograph of 60Sn-40Pb sample on Cu failed
in tension. XBB 862-1245A.

LAWRENCE BERKELEY LABORATORY
CENTER FOR ADVANCED MATERIALS
1 CYCLOTRON ROAD
BERKELEY, CALIFORNIA 94720